Applied Food Research 6 (2026) 102456

Contents lists available at ScienceDirect

Applied Food Research

journal homepage: www.elsevier.com/locate/afres

Purification with XAD-16 resin intensifies the polyphenolic composition, antioxidant potential, and anti-obesity properties of apple peel extracts

Nikoo Ostovar [a], Carolina Girotto Pressete [a,b], Fahrul Nurkolis [c], Lusânia Maria GreggiAntunes [b], Fabiana Andrea Hoffmann Sarda [a], George Barreto [a], Daniel Granato [a,d,*]

[a] Bioactivity & Applications Laboratory, Department of Biological Sciences, Faculty of Science and Engineering, University of Limerick, V94 T9PX, Limerick, Ireland
[b] Department of Clinical Analysis, Toxicology and Food Science, School of Pharmaceutical Sciences of Ribeirão Preto, University of São Paulo, CEP, 14040-903, Ribeirão Preto, Brazil
[c] Department of Biological Sciences, State Islamic University of Sunan Kalijaga (UIN Sunan Kalijaga), Yogyakarta, Indonesia
[d] Department of Biomedical, Chemical, and Food Sciences, School of Science, Faculty of Health and Environmental Science, Auckland University of Technology, 34 Saint Paul Street, Auckland Central, 1010, New Zealand

ARTICLE INFO

Keywords:
Sustainability
Polyphenols
Hemolysis
Copper-induced plasma oxidation
Human erythrocytes
HepG2 cells
ROS generation
Spheroids
Chemical stability

ABSTRACT

Apple peel (AP) is a rich source of polyphenols with potential applications in functional food development. This study investigated the optimization of green ultrasound-assisted extraction of polyphenols from Red Prince apple peel using response surface methodology (RSM), evaluating the effects of ultrasound power, ethanol concentration, and solid-to-solvent ratio on extraction efficiency and polyphenol bioactivity. The optimal extraction conditions consisted of a 1:15 solid-to-solvent ratio, 500 W ultrasound power, and 50% ethanol. The crude extract (CE) was subsequently purified using XAD-16 resin. Purification increased total phenolic, anthocyanin, and tannin contents by 28-, 6-, and 19-fold, respectively. The main phenolic compounds in the purified extract (PE) were hyperoside (16.65 mg/g), procyanidin B2 (9.59 mg/g), and epicatechin (8.50 mg/g). Both CE (30–300 mg/L) and PE (1–10 mg/L) protected erythrocytes against AAPH-induced hemolysis. PE markedly reduced ROS generation at 10 mg/L; however, at lower concentrations (1–2 mg/L), ROS levels increased, suggesting a potential pro-oxidant effect. In 2D HepG2 cultures, the CE extract was non-cytotoxic at 5–300 μg/mL and reduced intracellular ROS production. In contrast, PE decreased HepG2 viability at 200–300 μg/mL and exhibited only a modest reduction in ROS generation at 5–100 μg/mL. In 3D HepG2 spheroids, both extracts decreased cell viability in a dose- and time-dependent manner and affected spheroid growth and structural integrity. Additionally, CE and PE showed dose-dependent inhibition of pancreatic lipase and HMG-CoA reductase, suggesting their potential to modulate obesity-related metabolic targets, with PE exhibiting stronger activity.

1. Introduction

In recent years, the management of agro-industrial waste has become a significant challenge for the food processing industry (Riaz et al., 2020). Developing innovative strategies to convert these by-products into value-added products is an effective way to reduce waste and promote a circular bioeconomy. At the same time, the prevalence of obesity has increased markedly worldwide. Obesity is a chronic disease characterized by adipose tissue inflammation, immune cell infiltration, and an imbalance between pro- and anti-inflammatory mediators (Ramírez-Moreno et al., 2022). This inflammatory state elevates the risk of cardiometabolic diseases and certain cancers (World Health Organization, 2024).

Phenolic compounds are potent plant-derived antioxidants that modulate inflammatory pathways, reduce oxidative damage to proteins, membrane lipids, and nucleic acids, and have significant potential for the prevention and management of obesity and other non-communicable diseases (Ramírez-Moreno et al., 2022). Apple processing generates large quantities of by-products, particularly apple peel (AP), which represent a valuable and underutilized source of phenolic compounds (Park et al., 2022). AP from the "Red Prince" cultivar, a red-skinned mutation of the Jonagold apple classified by the Organization for Economic Co-operation and Development (OECD) as a variety exhibiting a pronounced blush, is particularly rich in polyphenolic

* Corresponding author.
E-mail addresses: Daniel.granato@aut.ac.nz, george.barreto@ul.ie (D. Granato).

https://doi.org/10.1016/j.afres.2026.102456
Received 24 May 2026; Received in revised form 15 July 2026; Accepted 27 July 2026
Available online 27 July 2026

compounds (Walkowiak-Tomczak et al., 2021; Xiang et al., 2017).

Among the available techniques for extracting polyphenols from plant materials, ultrasound-assisted extraction (UAE) is particularly attractive because it is simple, cost-effective, and highly efficient. Its yield depends on factors such as time, temperature, solvent composition, and ultrasound parameters. (Hiranpradith et al., 2025). Ultrasound enhances extraction through cavitation, where collapsing microbubbles disrupt cell walls, improve solvent penetration, and increase mass transfer. These characteristics make the UAE an efficient and sustainable extraction technique.(Sette et al., 2024).

UAE can be used to obtain crude extracts (CE) using various solvents. However, crude plant extracts often contain non-bioactive compounds such as sugars, proteins, and pigments that may dilute the activity of target phytochemicals. Therefore, purification strategies are required to enrich bioactive compounds and enhance their functional properties for potential food and nutraceutical applications(Mohammadi, Guo et al., 2024). Macroporous resins are widely used to purify crude extracts from polyphenolic sources due to their high surface area, strong adsorption capacity via noncovalent interactions, chemical stability, rapid adsorption, low cost, and reusability (Dai et al., 2022). Amberlite® XAD-16 resins, a type of styrene-divinylbenzene copolymer, primarily capture phenolic substances through hydrophobic and π–π interactions (Diemer et al., 2026). It possesses a high specific surface area (~800 m^2/g) and an average pore diameter of approximately 200 Å, facilitating the adsorption of low- and medium-molecular-weight phenolics. The adsorption behavior of individual phenolic compounds is influenced by their molecular size, polarity, degree of glycosylation, and structural conformation, which determine their affinity toward the resin matrix (Gong et al., 2022). Accordingly, the high surface area and selective adsorption capacity of macroporous resins enable the enrichment of phenolic compounds from crude extracts, yielding purified extracts with greater concentrations of bioactive constituents and, potentially, enhanced antioxidant and functional properties (Köpsel et al., 2025).

Despite the well-documented antioxidant properties of polyphenols from AP (Giomaro et al., 2014; Wolfe et al., 2003), most previous studies have focused on isolated pure compounds or have evaluated antioxidant capacity solely using chemical assays (Mantiniotou et al., 2024; Park et al., 2022), thus overlooking the potential synergistic effects of complex phenolic mixtures present in food-grade extracts. This highlights a critical gap in understanding the full biological potential of such extracts in physiologically relevant systems. Moreover, although AP has been incorporated into various food matrices, few studies have systematically validated the safety and efficacy of the extracted compounds through biologically relevant assays. To address these gaps, it is essential to investigate the anti-obesity activity of AP extracts and to comprehensively evaluate their cytotoxicity and antioxidant activity using in vitro cell-based models. Therefore, this study presents an integrated strategy that combines green ultrasound-assisted extraction, resin-assisted polyphenol enrichment, and advanced biological evaluation of AP polyphenols. To the best of our knowledge, it is the first to employ 3D HepG2 spheroid models to investigate the biological functionality of AP-derived polyphenols, establishing a more physiologically relevant platform for assessing their antioxidant and metabolic bioactivities and supporting their valorization as functional food ingredients.

2. Materials and methods

2.1. Chemical reagents

Ethanol (99% purity, analytical grade) was acquired from Fisher Scientific (Thermo Fisher Scientific Inc., Waltham, MA, USA), and Amberlite XAD-16 resin was obtained from Thermo Scientific (Thermo Fisher Scientific Inc., Waltham, MA, USA). Iron (II) sulfate heptahydrate, citric acid, sodium nitrite, aluminum chloride hexahydrate, sodium hydroxide, hydrogen peroxide, ammonium acetate, and sodium chloride were obtained from Scientific Laboratory Supplies (Dublin, Ireland). Folin-Ciocalteu phenol reagent, catechin, ferulic acid, quercetin, 1,10-phenanthroline, neocuproine, ascorbic acid, vanillin, HPLC-grade acetonitrile, 2′,7′-dichlorofluorescin diacetate (DCFH-DA), sodium carbonate, fetal bovine serum (FBS), resazurin, and penicillin were purchased from Sigma-Aldrich (Steinheim, Germany). Sodium phosphate monobasic monohydrate, sodium (mono)hydrogen phosphate, gallic acid, potassium chloride, sodium acetate, copper (II) chloride dihydrate, hydrochloric acid, formic acid, and sulfuric acid were obtained from Fluka (Muskegon, MI, USA). The HPLC standards (>98% purity) of (–)-epicatechin, chlorogenic acid, procyanidin B2, cyanidin-3-galactoside, hyperoside, and phlorizin were purchased from Extrasynthese (Genay, France). 2,2′-azobis(2-amidinopropane) dihydrochloride (AAPH), dimethyl sulfoxide (DMSO), and 3-(4,5-dimethylthiazol-2-yl)-2,5-diphenyl tetrazolium bromide (MTT) were obtained from Merck KGaA (Darmstadt, Germany). HPLC-grade methanol was obtained from Chem-Lab NV (Belgium). The HepG2 cell line was purchased from the American Type Culture Collection (ATCC, Rockville, MD, USA). Normal melting point agarose (NMP) was obtained from Invitrogen, Thermo Fisher Scientific (Carlsbad, CA, USA). Recombinant human 3-hydroxy-3-methylglutaryl-CoA reductase (HMGCR), nicotinamide adenine dinucleotide phosphate (NADPH), and porcine pancreatic lipase were obtained from Sigma-Aldrich (St. Louis, MO, USA).

2.2. Pre-treatment of red prince apple peel by-product

Fresh AP, a by-product of industrial apple juice production, was kindly supplied by Con Traas Ltd. (The Apple Farm, Tipperary, Ireland) and was immediately sealed in plastic bags and stored at −20 °C before further processing. To determine their dry matter content using Eq. (1), the fresh peels were dried in an oven at 50 °C for 48 h, then ground into a fine powder. The resulting powder was stored at room temperature in polyethylene bags, prepared for subsequent extraction experiments.

$$\text{Dry matter content}\left(\frac{w}{w}\ \%\right) = \frac{\text{Weight of dried AP (g)}}{\text{Weight of fresh AP (g)}} \times 100 \quad (1)$$

2.3. Extraction of bioactive compounds

A Box-Behnken design was employed to optimize the UAE of bioactive compounds. The independent variables included ultrasound power levels (250 W, 375 W, and 500 W), ethanol concentrations in water acidified with 0.05 mol/L citric acid (50%, 75%, and 100%), and solid-to-solvent ratios (1:15, 1:30, and 1:45, g: mL). The extraction was performed for 10 min using a Fisher Scientific (USA) instrument operating at 20 kHz. The mixtures were then centrifuged at 4000 rpm for 5 min. The experimental design consisted of 15 combinations (Table 1), with 4 replicates at the central point used to estimate the pure error of the proposed models. Duplicate extracts were prepared and pooled for further analyses.

2.4. Characterization of the apple peel extracts

2.4.1. Phenolic composition of extracts

The total phenolic content (TPC) was determined in quadruplicate using Folin-Ciocalteu reagent through a 96-well microplate reader, following established standard protocols, and the results were reported as mg of gallic acid equivalents per 100 g of AP (mg GAE/100 g) (Margraf et al., 2015). For the total monomeric anthocyanin content (TAC), the absorbance of the diluted sample was measured in pH 1.0 and pH 4.5 buffers at 520 and 700 nm, using distilled water as the reference. The TAC results were expressed as mg of cyanidin-3-glucoside equivalents per 100 g of AP (mg CYE/100 g) (Lee et al., 2005). To assay the total flavonoid content (TFC), the extract was mixed with solutions of 0.5 mol/L sodium nitrite, 0.3 mol/L aluminum chloride, and 1 mol/L sodium hydroxide (Mohammadi, Guo et al., 2024). The TFC values were

Table 1
Effect of ultrasonic power, solid-to-liquid ratio, and ethanol concentration on chemical composition and antioxidant capacity of Red Prince apple peel extracts.

Sample	Ultrasound Power (W)	1:X (mL)	Ethanol %	TPC (mg GAE/ 100 g)	TFC (mg CTE/ 100 g)	CT (mg CTE/ 100 g)	TAC (mg CYE/ 100 g)	HRSA (mg GAE/ 100 g)	CUPRAC (mg AAE/ 100 g)	Colour intensity (a. u.)	Red pigments (%)
1	250	1:15	75	513±13^{b}	418±8^{b}	1102±11^{ab}	3.36±0.32^{a}	75±19^{a}	3118±65^{ab}	0.36±0.02^{b}	30±0.34^{b}
2	500	1:15	75	502±14^{bc}	401±7^{b}	1036±83^{ab}	3.32±0.49^{a}	77±2	2713±17^{c}	0.79±0.07^{a}	33±1.81^{a}
3	250	1:45	75	472±31^{b}	140±<1^{i}	1612±301^{a}	0.65±0.29^{a}	60±6	3112±26^{ab}	0.12±0.01^{d}	29±0.76^{b}
4	500	1:45	75	539±30^{ab}	205±22 *g*	1427±191^{a}	0.82±0.31^{a}	75±5^{a}	3119±78^{ab}	0.12±0.01^{d}	30±0.48^{b}
5	250	1:30	50	622±38^{a}	359±8^{c}	1121±52^{ab}	1.18±0.05^{a}	40±3^{abc}	3245±35^{a}	0.16±0.01^{d}	35±0.32^{a}
6	500	1:30	50	637±29^{a}	375±8^{bc}	1281±95^{ab}	1.15±0.11^{a}	41±1^{abc}	3258±38^{a}	0.17 ±<0.01^{d}	35±0.27^{a}
7	250	1:30	100	304±11^{d}	112±8^{i}	812±68 ^{bc}	1.29±0.20^{a}	18±2^{abcd}	724±17^{f}	0.12±0.01^{d}	21±1.27^{c}
8	500	1:30	100	312±6^{d}	108±<1^{i}	702±86 ^{bc}	0.63±0.12^{b}	51±4^{ab}	1562±67^{d}	0.12±0.01^{d}	22±0.71^{c}
9	375	1:15	50	592±12^{a}	429±7^{f}	1024±124 ^{ab}	2.68±0.22^{a}	38±2^{abc}	3113±38^{ab}	0.28±0.01^{c}	34±0.21^{a}
10	375	1:45	50	559±25^{ab}	254±1^{b}	1308±123^{a}	0.68±0.13^{a}	21±2^{abcd}	2977±94^{b}	0.14±0.01^{d}	34±0.50^{a}
11	375	1:15	100	278±14^{d}	157±12^{h}	526±77 ^{c}	2.15±0.93^{a}	66±4^{a}	1472±23de	0.24±0.03^{c}	23±2.55^{c}
12	375	1:45	100	268±21^{d}	112±3^{i}	1263±91^{ab}	0.81±0.20^{a}	37±5^{abc}	1686±52^{d}	0.09±0.01^{d}	22±1.27^{c}
13	375	1:30	75	552±40^{ab}	386±14^{bc}	1750±140^{a}	1.24±0.39^{a}	50±4^{abc}	3385±138^{a}	0.19±0.01^{cd}	30±0.43^{b}
14	375	1:30	75	488±11^{bc}	310±<1^{e}	1367±140^{a}	1.26±0.49^{a}	52±2^{ab}	3015±96^{b}	0.19±0.02^{cd}	30±0.48^{b}
15	375	1:30	75	560±17^{ab}	347±14^{cd}	1321±100^{a}	0.92±0.55^{a}	51±^{ab}	3155±35^{ab}	0.17±0.01^{d}	30±<1^{b}
OPT	500	1:15	50	680±18 ^{a}	615±24^{a}	999±91^{ab}	1.89±0.26 ^{b}	41±3 ^{bc}	3242±58^{a}	0.24±0.01^{c}	29±1^{b}

Note: OPT = optimal extract; TPC = total phenolic content; TFC = total flavonoid content; = CT = condensed tannin content; TAC = total anthocyanin content; HRSA = hydroxyl radical scavenging activity; GAE = gallic acid equivalent; CTE = catechin equivalent; CYE = Cyanidin-3-glucoside equivalent; EDTAE = EDTA equivalent; AAE = ascorbic acid equivalent. Different superscript letters in the same column represent statistically different ($p < 0.05$) results.

expressed as mg of catechin equivalents per 100 g of AP (mg CTE/100 g). The condensed tannin content (CT) was determined using a vanillin-based assay that relies on the reaction between vanillin and CT, and results were expressed as mg of (+)-catechin equivalents per 100 g of AP (mg CE/100 g) (Fidelis et al., 2018).

2.4.2. *In vitro antioxidant capacity*

The antioxidant properties of the extract were evaluated using various chemical-based methods, as described by Pap et al. (2021). To determine the hydroxyl radical-scavenging activity, the diluted extract was mixed with iron (II) sulfate heptahydrate (1 mmol/L), hydrogen peroxide (15 mmol/L from a 30% H_2O_2 solution), and 1,10-phenanthroline (1 mmol/L). Results were expressed in mg of gallic acid equivalents per 100 g of AP.

For the cupric ion-reducing antioxidant capacity (CUPRAC), the extract was reacted with $CuCl_2$ (1.0×10^{-2} mol/L), neocuproine (7.5×10^{-3} mol/L), and ammonium acetate buffer (1 mol/L, pH 7.0). Absorbance was measured at 450 nm after 30 min of incubation at room temperature, and the results were expressed as mg of ascorbic acid equivalents per 100 g of AP (mg AAE/100 g).

2.4.3. *Instrumental color of apple peel extract*

The instrumental color of the extract was analyzed by measuring its maximum absorbance at 420 nm (yellow pigments), 520 nm (red pigments), and 620 nm (blue pigments) using spectrophotometry. These values were then used to calculate color intensity (CI) and the relative percentages of yellow, red, and blue pigments using Eqs. (2)–5:

$$CI = A_{420nm} + A_{520\ nm} + Abs_{620nm} \quad (2)$$

$$YP = 100 \times [(A_{420nm})/CI] \quad (3)$$

$$RP = 100 \times [(A_{520nm})/CI] \quad (4)$$

$$BP = 100 \times [(A_{620nm})/CI] \quad (5)$$

2.5. *Response surface modeling and optimization of the extraction conditions*

Experimental data were analyzed using response surface methodology (RSM) to construct a mathematical model describing the relationship between key independent variables (ultrasonic power, solid-to-solvent ratio, and ethanol concentration, denoted as x_i, x_j, and x_k) and the corresponding response variables of Red Prince AP extracts (Farrell et al., 2024). A second-order polynomial model was employed to describe the relationships between the independent variables and the measured responses. The model included linear, quadratic, and interaction terms, as expressed in Eq. (6):

$$Y = \beta_0 + \sum_{i=1}^{k} \beta_i X_i + \sum_{i=1}^{k} \beta_{ii} X_i^2 + \sum_{i=1}^{k-1} \sum_{j=i+1}^{k} \beta_{ij} X_i X_j + \varepsilon \quad (6)$$

ANOVA method applied to assess the significance of the fitted models and regression coefficients. Regression terms with $p < 0.10$ were retained in the final RSM models. Model adequacy was assessed using the coefficient of determination (R^2) and adjusted R^2 values calculated in TIBCO Statistica (version 13.1; TIBCO Statistica Inc., Palo Alto, CA, USA). Models with R^2 values greater than 0.70 were considered satisfactory.

2.6. *Effect of pH on the stability of anthocyanins and antioxidant capacity*

The influence of pH on the stability and reversibility of anthocyanins in the optimized AP extract was assessed over the pH range of 2 to 8, following the method described elsewhere (Escher et al., 2018). The extract was diluted with ultrapure water acidified with HCl to pH 2, yielding an absorbance of approximately 0.80 at 525 nm. A gradual titration with 2.0 mol/L NaOH was then carried out in a beaker under magnetic stirring and with light protection, until pH levels of 4, 6, and 8 were reached. At each pH level, absorbance at 525 nm was measured. This was followed by a reverse titration with 1.0 mol/L HCl to restore the pH to 2. The CUPRAC method and instrumental color were also evaluated. UV–Vis spectra of each extract were recorded over the wavelength range 450 nm to 700 nm. Reversibility (%) was determined by comparing the absorbance at 525 nm after the pH was returned to 2 with the initial absorbance at pH 2.

2.7. *Purification of crude extract using amberlite® XAD-16 resin*

Optimal extract was prepared by mixing 2 g of dried AP with 30 mL of 50% ethanol in acidified water (0.05 mol/L citric acid), then sonicated at 20 kHz and 500 W for 10 min in four true replicates. Then the

samples were centrifuged at 4500 rpm for 5 min, and the supernatant was collected and filtered through Whatman No 1 filter paper. The filtrate was concentrated by rotary evaporation to remove the solvent. The extract was freeze-dried at −70 °C to preserve the stability of thermolabile bioactive compounds prior to further analysis (Shakoor et al., 2023). This low-temperature drying method minimizes thermal degradation and oxidative changes, facilitating the storage and characterization of the polyphenol-rich extract. The extract weight was measured, and the samples were stored at −20 °C until further analysis. Minor modifications were applied to the purification method reported by Mohammadi et al.(Mohammadi, Guo et al., 2024). Briefly, 1.5 g of optimized freeze-dried CE was dissolved in 5 mL of acidified water (pH 2) adjusted with concentrated HCl, and the mixture was stirred until completely dissolved in 5 replicates. The Amberlite XAD-16 resin was then added at a 1:5 (w/w) ratio (extract: resin), and the mixture was stirred for 2 h. The solution was loaded onto a glass column (1.0 cm diameter × 20.0 cm length). The column was first washed with 300 mL of acidified water (pH 2) to remove organic acids, polysaccharides, and other non-phenolic impurities. This was followed by a 300 mL rinse with distilled water to flush out remaining extract components. The phenolic-rich fraction was then eluted using 250 mL of absolute ethanol. Then, the solvent was evaporated at 40 °C to obtain the PE, which was stored at −20 °C in a light-protected container. The yield was determined using Eqs. (7,8):

$$\text{The yield of CE } \left(\frac{w}{w}\%\right) = \frac{\text{Weight of freeze} - \text{dried powder (g)}}{\text{Weight of dried sample (g)}} \times 100 \quad (7)$$

$$\text{The yield of PE } \left(\frac{w}{w}\%\right) = \frac{\text{Weight of Purified powder (g)}}{\text{Weight of Crude powder (g)}} \times 100 \quad (8)$$

The recovery (%) of polyphenols after purification was determined using a mass balance approach based on Eq. (9):

$$\text{Recovery (\%)} = \frac{C_{purified} \times Y}{C_{crude}} \times 100 \quad (9)$$

Where $C_{purified}$ and C_{crude} represent the target bioactive content in the purified fraction and crude extract, respectively, and Y is the mass yield of the purified extract relative to the crude extract.

2.8. Characterization of the optimal red prince apple peel extract

2.8.1. Chemical composition and antioxidant potential

The bioactive compounds and antioxidant capacity of CE and PE, prepared under optimal conditions, were analyzed as described in Section 2.4. Phenolic compounds in CE and PE were quantified in triplicate using an Agilent 6230 LC-TOF system (Farrell et al., 2024). Extract (3 mg) was dissolved in 1 mL of 50% ethanol and filtered through a 0.45 µm membrane. A 10 µL sample was injected onto a Zorbax SB-C18 column (150 mm × 4.6 mm, Agilent) maintained at 40 °C. The mobile phase consisted of solvent A (water with 0.1% formic acid, v/v) and solvent B (HPLC-grade acetonitrile). The gradient program started with 5% B, increased to 8% at 20 min, 12% at 34 min, 16% at 43 min, and 30% at 55 min, then returned to 5% at 60 min. The flow rate was set to 1 mL/min. Phenolic compounds were detected at 280, 320, 360, and 520 nm using the DAD. Identification relied on matching retention times and UV spectra with those of reliable standards. In contrast, quantification was carried out using calibration curves for each analyte, taking into account linearity as well as the limits of detection (LOD) and quantification (LOQ): gallic acid (5–50 mg/L, R^2 = 1, LOD=0.290 mg/L, LOQ=0.879 mg/L), (+)-catechin (5–50 mg/L, R^2 = 1, LOD=0.571 mg/L, LOQ=1.729 mg/L), chlorogenic acid (5–50 mg/L, R^2 = 0.997, LOD=3.574 mg/L, LOQ=10.830 mg/L), cyanidin-3-galactoside (5–50 mg/L, R^2 = 0.999, LOD=0.029 mg/L, LOQ=0.089 mg/L), procyanidin B2 (5–50 mg/L, R^2 = 0.999, LOD=0.595 mg/L, LOQ=1.804 mg/L), (–)-epicatechin (5–50 mg/L, R^2 = 0.999, LOD=0.569 mg/L, LOQ=1.724 mg/L), ferulic acid (5–50 mg/L, R^2 = 1, LOD=0.576 mg/L, LOQ=1.745 mg/L), hyperoside (5–50 mg/L, R^2 = 1, LOD=0.178 mg/L, LOQ=0.539 mg/L), and phlorizin (5–50 mg/L, R^2 = 1, LOD=0.287 mg/L, LOQ=0.869 mg/L).

To assess the inhibition of copper-induced oxidation in human plasma, a blood sample (v = 8 mL) from a healthy participant was collected by a professional phlebotomist after the project protocols were reviewed and approved by the Science and Engineering Research Ethics Committee (approval #2023_02_01_S&E and #2025_05_07_S&E).

Plasma was obtained by centrifugation at 1200 g for 10 min to separate red blood cells (RBC) (Franchin et al., 2025). In a 96-well UV plate, 50 µL of phosphate-buffered saline (PBS; 26.5 mmol/L phosphate, 137 mmol/L NaCl, pH 7.4) and two concentrations of each extract were mixed, in quadruplicate, with 50 µL of plasma diluted 40-fold in PBS. The mixtures were incubated at 37 °C for 15 min. Lipid oxidation was then initiated by adding 100 µL of $CuCl_2$ (150 µM in PBS). PBS served as the positive control (maximum plasma oxidation), while plasma without $CuCl_2$ was used as the negative control. The formation of conjugated dienes was monitored by measuring absorbance at 245 nm every 3 min for 120 min at 37 °C (Granato, 2026). Antioxidant capacity was quantified using an ascorbic acid calibration curve (0–20 mg/L, n = 4, R^2 = 0.985) and expressed as mg ascorbic acid equivalents per g (mg AAE/g). The lipoperoxidation rate at different concentrations of CE and PE was determined by linear regression analysis, with absorbance at 245 nm plotted against time (min). Antioxidant activity of ascorbic acid concentrations was represented by the slope of the regression line, indicating the ability to suppress lipid peroxidation. Antioxidant activity, expressed as the lipoperoxidation rate, was calculated from the slope of the regression analysis and expressed as Abs_{245nm} /min:

$$v = \frac{\Delta Abs_{245nm}}{\Delta t} \quad (10)$$

The lipid peroxidation inhibition rate (%) was calculated according to Eq. (11):

$$\text{Inhibition rate (\%)} = \left(1 - \frac{v_{sample}}{v_{PC}}\right) \times 100 \quad (11)$$

Where v_{sample} is the oxidation rate of the sample, and v_{PC} is the oxidation rate of the positive control.

2.8.2. Evaluation of erythrocyte antioxidant capacity and antihemolytic activity

The ability of CE and PE to scavenge hydroxyl radicals was investigated using the erythrocyte hemolysis method outlined by Mohammadi et al.(Mohammadi, Guo et al., 2024). In this assay, 100 µL of RBCs (20% haematocrit diluted in PBS [5 mmol/L phosphate, 154 mmol/L NaCl, pH 7.4]) were mixed with either PBS, quercetin at 95 mg/L (reference compound), or three concentrations of CE and PE (prepared in PBS according to their TPC values). The mixtures were placed in 2 mL microtubes and pre-incubated at 37 °C with agitation (150 rpm, Stuart SI500, Reagecon Diagnostics Ltd., Shannon, Ireland) for 20 min. Then, 200 µL of AAPH solution (200 mM in PBS) was added, and the reaction was allowed to proceed under the same conditions for 2 h to induce oxidative hemolysis. The positive control had 100 µL RBCs, 100 µL PBS, and 200 µL AAPH, and represented the condition of maximal oxidative stress. The negative control consisted of 100 µL RBCs and 300 µL PBS, and served as the minimal oxidation.

Following treatment, the suspensions were centrifuged (1200 g, 10 min, 4 °C). The supernatant was used to determine hemolysis, while the cell pellets were reserved for measuring intracellular ROS levels. To quantify hemolysis, 100 µL of the supernatant was diluted with 200 µL of PBS, and absorbance was read at 540 nm (Absorbance A) using a microplate reader. Complete hemolysis was determined by mixing 100

μL of RBCs in PBS with 300 μL of ultrapure water, and measuring the absorbance at 540 nm (Absorbance B). The percentage of hemolysis inhibition was calculated as described in Eq. (12):

$$\textit{Inhibition of hemolysis}(\%) = \left(1 - \frac{A}{B}\right) \times 100 \quad (12)$$

Cellular antioxidant activity was evaluated using DCFH-DA. The cell pellets were washed twice with 400 μL of PBS, then centrifuged at 1200 g for 3 min at 4 °C. Then, cells were resuspended in 400 μL of a 10 μmol/L DCFH-DA solution, and 300 μL of this suspension was transferred to a microplate and incubated at 37 °C in the dark for 20 min. PBS-treated cells were used as the negative control and exhibited the highest intracellular ROS levels. The effects of the CE and PE on ROS generation were subsequently evaluated at the selected concentrations. ROS levels were determined by measuring the fluorescence intensity at an excitation wavelength of 485 and an emission wavelength of 520 nm using a microplate reader. Experiments in RBC were analysed in technical quadruplicates.

2.8.3. Cytotoxic and cellular antioxidant activity in human-derived cell lines

2.8.3.1. Cell lines, culture cell conditions, and treatment schedule. The hepatocellular carcinoma cell line HepG2 was cultured in Dulbecco's Modified Eagle's Medium (DMEM) supplemented with 10% fetal bovine serum and 1% antibiotic-antimycotic solution (10,000 units/mL penicillin, 10,000 μg/mL streptomycin, and 25 μg/mL amphotericin B). Cells were maintained in a 3110 Series II CO_2 water-jacketed incubator (Thermo Fisher Scientific, Carlsbad, CA, USA) at 37 °C in a humidified atmosphere containing 5% CO_2 and 96% relative humidity. All culture procedures followed the recommendations of Bal-Price & Coecke (2011). CE and PE were solubilized in a 20% (v/v) dimethyl sulfoxide (DMSO), and 80% (v/v) Milli-Q water mixture, and the stock solution (10,000 μg/mL) was stored at −20 °C until use. Immediately before treatment, the extracts were freshly diluted in culture medium to obtain the desired final concentrations.

2.8.3.2. Tumor spheroids culture. HepG2 tumor spheroids were generated using the agarose-coated overlay method, as described by Friedrich et al. (2009). Briefly, 96-well plates (Greiner Bio-One; Monroe, NC, USA) were coated with 2% normal-melting-point agarose prepared in PBS. After agarose solidification, HepG2 cells (2×10^3) suspended in complete culture medium were seeded into each well using a micropipette. The plates were then transferred to the incubator and maintained undisturbed for 96 h to allow tumor spheroid formation (initiation phase). Spheroid integrity and growth kinetics were initially monitored during the first 72 h of exposure to CE and PE, and subsequently every 48 h, by analyzing images acquired with a phase-contrast microscope (Carl Zeiss, Germany).

2.8.3.3. Effects of crude and purified extracts on hepg2 cell viability and cellular antioxidant activity (monoculture). Cell viability was assessed using the 3-(4,5-dimethylthiazol-2-yl)-2,5-diphenyltetrazolium bromide (MTT) assay according to Garcia et al. (2024). The cells were treated with DMEM (NC-negative control), 0.5% v/v DMSO (SC-solvent control), or CE and PE (5–300 μg/mL) in quadruplicate for 24 h to determine IC_{50} values. Following treatment, 10% MTT solution (5 mg/mL) was added to each well, and after 4 h of the MTT reaction, the medium was discarded and replaced with 50 μL of DMSO. Absorbance was measured at 570 nm using a microplate reader, and the data were presented as the mean ± standard deviation (SD) from two independent experiments.

Intracellular ROS-scavenging activity of CE and PE was assessed in HepG2 cells (1×10^4 cells/well) using the DCFH-DA assay, following the manufacturer's recommendations and as previously reported by Prieto et al. (2013). Cells were exposed to the extracts at concentrations of 5, 50, and 100 μg/mL in quadruplicate for 24 h, then incubated with 5 μmol/L DCFH-DA at 37 °C in the dark for 30 min. Oxidative stress was then induced by adding 1 mmol/L H_2O_2 for 20 min. The negative control consisted of cell culture medium without H_2O_2. The fluorescence intensity was recorded at $\lambda_{excitation} = 450$ nm and $\lambda_{emission} = 520$ nm, and results were expressed as a percentage of the fluorescence intensity relative to the positive control. Two independent experiments were performed, each with three technical replicates, and the results are presented as the mean ± standard deviation.

2.8.3.4. Cell viability assay (3D spheroid). The resazurin assay was performed according to the protocols described by Riss et al. (2011); Walzl et al. (2014). After the initiation phase, HepG2 spheroids were treated with DMEM (NC), DMSO (SC), or CE and PE at concentrations of 100, 200, and 300 μg/mL for 24, 48, 72, 120, and 168 h. Subsequently, a resazurin working solution (0.15 mg/mL in PBS) was added to each well at 20% of the final volume, containing the tumor spheroids. The plates were incubated at 37 °C for 72 h, and absorbance was measured using a microplate reader (Biotek ELx800) at λ = 570 nm for resorufin and λ = 600 nm for resazurin. Absorbance values were corrected by multiplying them by the oxidation factor at each wavelength and subtracting the contribution of converted resorufin. Cell viability (%) was calculated by normalizing the absorbance values for each treatment to the negative control, which was set to 100% viability. All analyses were performed using twelve spheroids per treatment (n = 12) in three independent biological experiments (n = 3).

2.8.3.5. Volume, morphology, and integrity analyses (3D spheroid). The volume, morphology, and integrity of HepG2 spheroids were evaluated according to the methods described by Friedrich et al. (2009); Vinci et al. (2012). After the initiation phase, photomicrographs of HepG2 spheroids were acquired using an AxioCam MRc image-capture system (Carl Zeiss; Göttingen, Germany) coupled to an inverted Axio LabA1 microscope (Carl Zeiss) with a 4× objective lens. Images were analyzed using AxioVision SE64 Rel. 4.9.1 software (Carl Zeiss). Following image acquisition, spheroids were treated with DMEM (NC), DMSO (SC), or CE and PE at concentrations of 100, 200, and 300 μg/mL. For morphology and integrity assessment, photomicrographs of each spheroid were recorded after 24, 48, 72, 120, and 168 h of treatment. Each image was evaluated to identify irregular spheroids (i.e., loss of circular shape) and evidence of cell disaggregation. For spheroid volume quantification, the circumference of each tumor spheroid was measured using the "measure" tool in AxioVision SE Rel. 4.9.1 software. The spheroid area was expressed in μm^2 and the diameter in μm. All analyses were performed using twelve spheroids per treatment (n = 12) in three independent biological experiments (n = 3).

2.8.4. Evaluation of anti-obesity potential of the optimal extract

2.8.4.1. In vitro lipase inhibition assay. Lipase inhibition was evaluated using porcine pancreatic lipase (PPL) at a concentration of 0.1 mg/mL, prepared in PBS (50 mM, pH 8) (Nayebhashemi et al., 2023). CE, PE, and Orlistat (25, 50, 75, 100, and 125 μg/mL) were added to a transparent 96-well microplate along with 20 μL of *p*-nitrophenyl butyrate (pNPB, 10 mM in buffer) and incubated at 37 °C for 10 min. The mixture was then vortexed and incubated to ensure complete dissolution before the assay. Absorbance was measured at 405 nm using a microplate reader. Enzyme activity was expressed as the rate of formation of 1 mol of *p*-nitrophenol ($C_6H_5NO_3$) per min at 37 °C. Lipase inhibition was calculated based on the decrease in PPL activity in the presence of test samples. All experiments were conducted in triplicate in three independent trials (n = 3), and percentage inhibition was determined using Eq. (13):

$$\textit{lipase Inhibition}\ (\%) = \left[1 - \frac{(B - \mathrm{Bc})}{(A - \mathrm{Ac})}\right] \times 100 \quad (13)$$

Where A = enzymatic activity without inhibitor, B = enzymatic activity with inhibitor, A_c = Negative control without inhibitor, B_c = Negative control with inhibitor. The IC_{50} values were determined by plotting the normalized lipase activity against the logarithm of the inhibitor concentration. The data were analyzed using GraphPad Prism 8.4.3 for Windows (GraphPad Software Inc., San Diego, CA, USA).

2.8.4.2. In vitro HMG-COA reductase inhibition assay. The inhibitory activity of CE and PE against human HMGCR was evaluated using a NADPH oxidation assay, as described elsewhere (Iqbal et al., 2014). Recombinant human HMGCR (0.1 U/mL) was prepared in PBS (100 mM, pH 7.4) containing 1 mM EDTA and 2 mM dithiothreitol. Test samples and simvastatin were initially dissolved in DMSO (100 mg/mL) and diluted in PBS to final concentrations of 25, 50, 75, 100, and 125 μg/mL, keeping DMSO ≤1%. In a 96-well microplate, 50 μL of enzyme solution was preincubated with 50 μL of sample or control (PBS as negative control) at 37 °C for 15 min. The reaction was initiated by adding 100 μL of substrate solution containing 0.15 mM HMG-CoA and 0.2 mM NADPH, and NADPH oxidation was monitored at 340 nm every 30 s for 10 min using a microplate reader. The initial reaction rate (ΔA_{340}/min) was calculated from the linear portion of the absorbance-time curve. Experiments were conducted in triplicate across three independent trials and reported as mean ± SD. Enzyme inhibition (%) was calculated using Eq. (14):

$$HMG-CoA\ Reductase\ Inhibition\ (\%) = \left[1 - \frac{Vsample}{Vcontrol}\right] \times 100 \qquad (14)$$

where $V_{control}$ and V_{sample} represent the reaction velocities in the absence and presence of the enzyme inhibitor, respectively. The IC_{50} values were determined by plotting the normalized HMG-Co reductase activity against the logarithm of the inhibitor concentration. The data were analyzed using GraphPad software.

2.9. Statistical analysis

All experiments were performed in three independent biological replicates, and each analytical determination was carried out in technical quadruplicate, where applicable. Results are expressed as mean ± standard deviation. Statistical analyses were conducted using TIBCO Statistica v.13.3 (Palo Alto, CA, USA). Differences among groups were evaluated by one-way analysis of variance (ANOVA), followed by Tukey's honestly significant difference (HSD) post hoc test when more than two groups were compared. Comparisons involving two groups were assessed using Student's *t*-test. Statistical significance was established at $p < 0.05$.

3. Results and discussion

3.1. Response surface modeling of extraction conditions for bioactivity and color

The extraction of bioactive compounds can be hindered by variations in their solubility and polarity of their chemical structures (Mantiniotou et al., 2024). Therefore, improving the efficiency of the extraction process is essential. The influence of ultrasonic power, solid-to-solvent ratio, and ethanol concentration on the chemical composition, color, and antioxidant capacity of Red Prince AP extract is summarised in Table 1. At the same time, the corresponding response surface models are presented in Fig. 1. The total phenolic content in AP ranged from 268 ± 21 to 637 ± 29 mg GAE/100 g, with the highest value obtained under extraction conditions of a 1:30 solid-to-solvent ratio, 500 W ultrasound power, and 50% ethanol concentration. The lowest TPC was obtained at a 1:45 solid-to-solvent ratio, 375 W ultrasound power, and 75% ethanol concentration. These values can be compared with previously reported values for optimized apple by-product extracts obtained using Soxhlet extraction with green solvents, where a maximum TPC of 11.90 g GAE/kg was reported using 80% ethanol and a 1:40 solid-to-solvent ratio (Villamil-Galindo & Piagentini, 2024). This value is lower than the maximum TPC observed in the present study, which may be attributed to the use of UAE extraction, in which cavitation enhances cell wall disruption and promotes the release of phenolic compounds. In contrast, Soxhlet extraction relies on continuous solvent reflux at elevated temperatures and longer extraction times. Higher TPC values have also been reported by Mantiniotou et al., who obtained 157–1593 mg GAE/g of AP using RSM to optimize multiple extraction techniques, including stirring, ultrasonication, and pulsed electric field-assisted extractions. These differences are likely due to variations in extraction methods and conditions such as temperature, time, and solvent composition (Mantiniotou et al., 2024).

The total flavonoid content of the samples ranged from 108 ± <1 to 429 ± 7 mg CTE/100 g. The highest flavonoid extraction was achieved using 50% ethanol, an ultrasonic power of 375 W, and a solid-to-solvent ratio of 1:15. These findings indicate that moderate solvent polarity and lower solvent dilution enhance flavonoid extraction. In a study on apple pomace, a TFC of 1.63 mg CTE/g was reported using 50% ethanol, an ultrasonic power of 500 W, and a 1:9 solid-to-solvent ratio. Despite differences in the sample matrix and extraction conditions, the TFC values obtained in the present study were generally higher (Mohammadi, Guo et al., 2024). Additionally, conventional

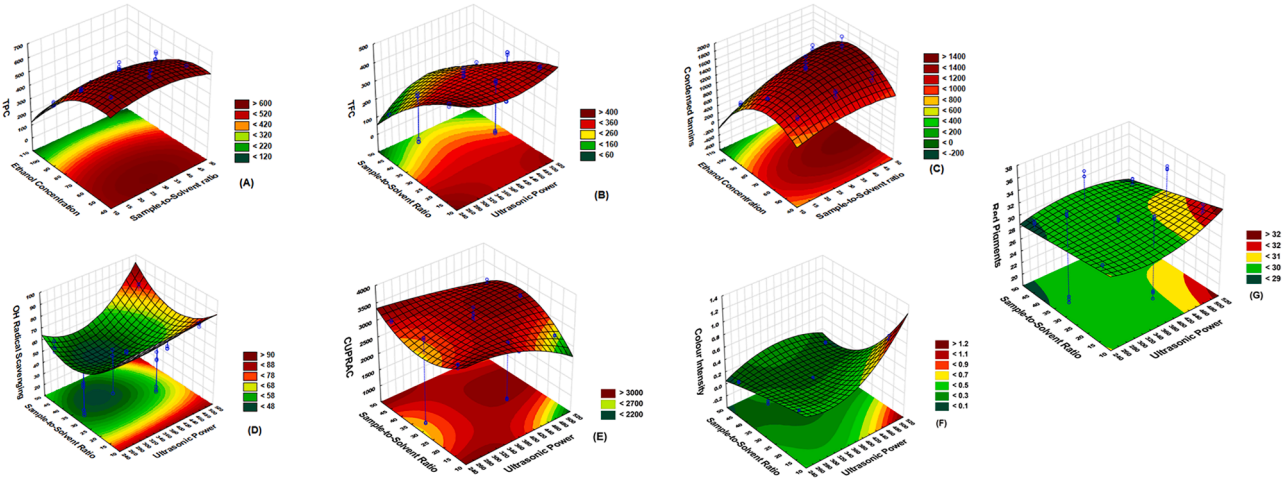

Fig. 1. Effect of ultrasound power (W), sample-to-solvent ratio, and ethanol concentration on total phenolic content (A), total flavonoid content (B), condensed tannins (C), hydroxyl radical scavenging activity (HRSA) (D), cupric-ion reducing antioxidant capacity (CUPRAC) (E), color intensity (F), and red pigments (G).

acetone-based extraction of AP using repeated homogenization and blending yielded TFC values of 306.1 ± 6.7 and 303.2 ± 41.5 mg CTE/100 g for the Rome Beauty and Idared cultivars, respectively. These values were lower than those obtained in the present study (Wolfe et al., 2003). These comparisons suggest that ultrasound-assisted extraction with ethanol can enhance flavonoid recovery from AP.

The RSM modeling (Table S1) revealed that ultrasonic power and solid-to-solvent ratio were the most influential factors governing both TPC and TFC, with higher power and lower ratios significantly enhancing extraction efficiency ($p < 0.05$). The fitted models explained 95.4% and 97.7% of the variability in TPC and TFC, respectively, demonstrating strong predictive performance.

The maximum condensed tannin content (1750 ± 140 mg CTE/100 g) was obtained under conditions of 375 W ultrasonic power, 75% ethanol, and a 1:15 solid-to-solvent ratio. Tannins in fruits consist of oligomeric and polymeric catechins (Zanchi et al., 2009). They are weakly acidic compounds that can develop partial charges through interactions with organic acids. Condensed tannins are typically much more soluble in ethanol and ethanol-water mixtures than in water alone. The RSM plots suggest that higher ultrasonic power, along with lower ethanol concentration and solid-to-solvent ratio, enhances the extraction efficiency of condensed tannins up to a certain threshold. This improvement is due to intensified cavitation, which improves mass transfer (Mohammadi, Franchin et al., 2024). The response surface showed a pronounced curving, indicating significant interaction between ethanol concentration and solid-to-solvent ratio. Maximum yields occurred at lower ratios and intermediate ethanol levels, suggesting optimized solvent polarity, whereas excessive ethanol reduced efficiency by limiting penetration and diffusion. Tannin yield also increased with the solid-to-solvent ratio up to a point, then declined at higher ratios. Huaman-Castilla et al. (2019). The model explained 84% of the variability, indicating satisfactory predictive performance.

Anthocyanin and red pigments extraction were strongly influenced by ultrasonic power, solid-to-solvent ratio, and ethanol concentration. The highest anthocyanin yields were achieved at low-to-moderate ultrasonic power, a low solid-to-solvent ratio, and an intermediate ethanol concentration. Under these conditions, TAC reached 3.36 ± 0.32 mg CYE/100 g, with a color intensity of 0.79 ± 0.0 a.u. and a red pigments percentage of approximately 35.0 ± 0.3%, suggesting efficient pigment release without excessive degradation. This effect is attributed to cavitation-enhanced cell disruption and solvent diffusion (Farrell et al., 2024). However, when ultrasonic power exceeded 500 W, color intensity and red pigments content were reduced due to anthocyanin degradation. The lower solid-to-solvent ratio improved pigment extraction by increasing solvent accessibility and concentration gradient (Shu et al., 2025). TAC and color extraction efficiency increased with ethanol proportion up to 75%, beyond which they declined sharply due to solvent polarity (Li et al., 2023). Anthocyanins are moderately polar, so an aqueous-ethanol mixture optimizes their solubility and stability. Furthermore, the slightly acidic extracting solution maintained them in the red, stable flavylium cation form, thereby avoiding cleavage of aromatic or aliphatic acyl linkages. Response surface plots (Fig. 1F-G) showed maximum color intensity and red pigments at high ultrasonic power and high solid-to-solvent ratios, and the models demonstrated excellent predictive accuracy ($R^2 = 0.994$ and 0.974).

Antioxidant capacity, measured by HRSA and CUPRAC assays, exhibited trends consistent with phenolic extraction efficiency. The hydroxyl radical scavenging activity varied from 18 ± 2 to 77 ± 2 mg GAE/100 g. The optimal conditions for HRSA were found at high ultrasonic power and intermediate-to-low sample-to-solvent ratios. The model exhibited a high coefficient of determination ($R^2 = 0.905$), showing its potential to explain the experimental results. The CUPRAC values ranged from 724 ± 17 to 3385 ± 138 mg AAE/100 g, which suggests that moderate ethanol concentrations efficiently extract both polar and nonpolar antioxidant compounds. This agreed with the principles of the CUPRAC assay, which determines antioxidant capacity through single electron transfer (SET) (Apak, 2018). As shown in the three-dimensional response surface (Fig. 1E), CUPRAC antioxidant activity increased markedly with increasing ultrasonic power up to an optimum level, indicating enhanced compound release due to ultrasonic disruption. Likewise, higher CUPRAC values were observed at lower solid-to-solvent ratios. These interactions indicate maximum recovery at intermediate power and solvent ratios, where mass transfer and stability are balanced. The model for CUPRAC activity exhibited excellent predictive accuracy ($R^2 = 0.984$).

The optimal extraction conditions for AP were 50% ethanol, 500 W ultrasonic power, and a 1:15 solid-to-solvent ratio. The physicochemical characteristics of the resulting extract are summarised in Table 1. The findings are consistent with previous reports indicating that 50% ethanol enhances phenolic extraction efficiency from AP (Park et al., 2022). To validate the predictive performance of the developed RSM models, predicted and experimental values, together with percentage deviations, are presented in Table 2. Good agreement was observed for TPC and CUPRAC, with deviations of 7% and 9%, respectively. Larger deviations were obtained for TFC, CT, and HRSA. However, the corresponding models exhibited satisfactory goodness-of-fit (R^2_{adj} values ranging from 0.84 to 0.99), while the overall desirability value of 0.81 indicated satisfactory simultaneous optimization of the evaluated responses. These findings demonstrate that the developed models adequately describe the influence of extraction parameters on the measured responses. However, reduced predictive accuracy was observed for some responses under the optimized conditions.

3.2. Anthocyanin reversibility with pH variation

The stability and color expression of anthocyanins in the optimized Red Prince AP extract were evaluated across a pH 2–8 using sequential acid-base titration (Fig. 2). Red pigments (RP) was highest at pH 2 (33.2%), reflecting predominance of the flavylium cation, then declined from pH 4–6 as yellow pigments increased, a pattern characteristic of partial anthocyanin degradation. At pH 6, RP remained at 30.7%, indicating a more balanced yellow-blue color due to the coexistence of multiple anthocyanin species. At pH 8, RP decreased to its lowest value (19.2 ± 0.1%), accompanied by a reduction in CUPRAC antioxidant capacity (2053 ± 62 mg/100 g). These changes are consistent with anthocyanin degradation into chalcones, phenolic acids, A-ring aldehydes, and other polymeric or oxidized products, depending on the anthocyanin structure (Enaru et al., 2021). The color shifted visibly from

Table 2
Experimental validation of the response surface methodology (RSM) models.

Response	−95% Predicted value	+95% Predicted value	Mean predicted value	Experimental value	Error (%)
TPC (mg GAE/ 100 g)	573	701	634	680	7
TFC (mg CTE/ 100 g)	475	561	518	615	19
CT (mg CTE/ 100 g)	1020	1628	1324.	999	25
HRSA (mg GAE/ 100 g)	50.13	77.40	63.77	41	36
CUPRAC (mg AAE/ 100 g)	3314	3789	3551	3242	9

Note: total phenolic content (TPC), total flavonoid content (TFC), condensed tannins (CT), hydroxyl radical scavenging activity (HRSA), cupric reducing antioxidant capacity (CUPRAC), gallic acid equivalent (GAE), catechin equivalent (CTE), and ascorbic acid equivalent (AAE).

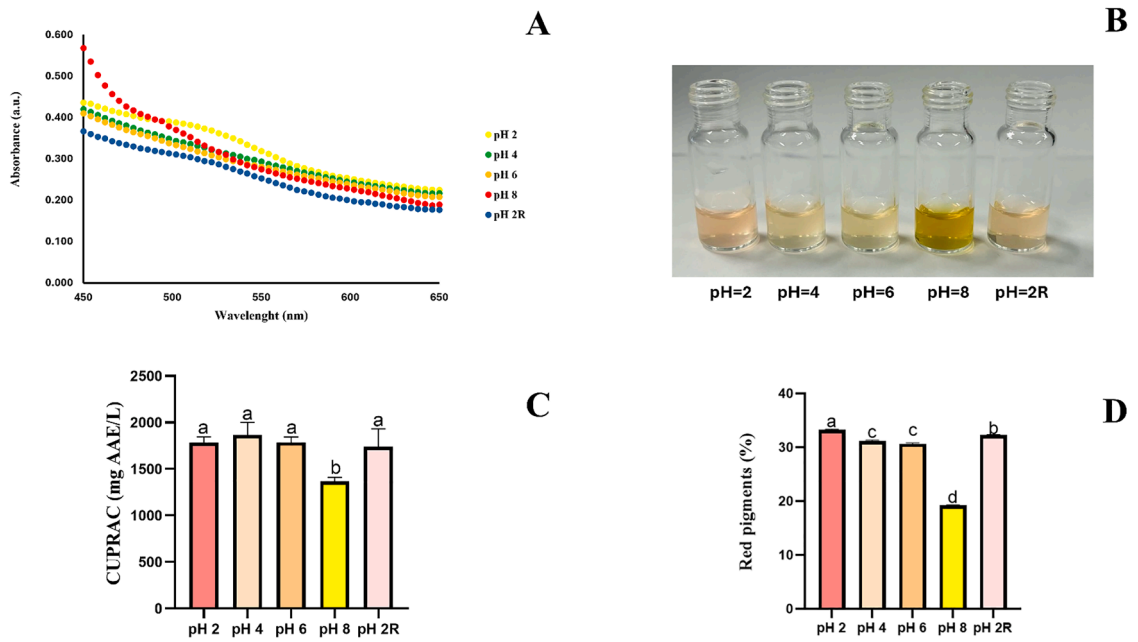

Fig. 2. Effect of different pH conditions (2, 4, 6, and 8) on the color intensity and antioxidant activity of the optimized anthocyanin extract from Red Prince apple peels. UV–Vis absorption spectra of the anthocyanin extract at different pH values and after pH reversibility treatment (pH 2R) (A), Color variation of the extract solutions under different pH conditions, showing the transition from red-pink coloration at pH 2 to a more pink-yellow coloration at pH 4 and yellow-green at pH 8 due to pH-dependent structural changes of anthocyanins. (B), CUPRAC antioxidant capacity of the extract at different pH levels, expressed as mg AAE/L (C), and retention (%) of red pigments at different pH values (D). Values are presented as mean ± standard deviation. Different letters comparing treatments represent statistically different means ($p < 0.05$).

light pink at pH 2 to yellow-green at pH 8, with statistically significant differences ($p < 0.05$). Reverse titration restored 80.4% of the red color, while antioxidant capacity remained unaffected, as CUPRAC values at pH 2 and 2R were statistically similar ($p > 0.05$). These results are consistent with previous reports on the pH-dependent stability of anthocyanins in blackberry and elderberry extracts (Mohammadi, Franchin et al., 2024). From an application perspective, the high reversibility and maintained antioxidant capacity at acidic pH values support the potential use of Red Prince AP extract as a functional colorant or antioxidant ingredient in acidic food matrices, such as beverages, yogurt, and fruit-based formulations. However, the marked instability observed at neutral to alkaline pH underscores the importance of pH control during processing and storage to preserve both color intensity and antioxidant performance.

3.3. *Effects of partial purification on the chemical composition of the optimal extract*

The effect of partial purification using Amberlite® XAD-16 resin on the chemical composition and antioxidant capacity of the optimally extracted Red Prince AP is presented in Table 3. The yields were 17.71% for dry matter content, 76.25% for CE, and 1.98% for PE. The recoveries (%) were approximately 55% for TPC, 38% for CT, and 13% for TAC. Partial purification resulted in a pronounced enrichment of phenolic constituents. TPC increased from 10 ± 1 mg GAE/g in CE to 276 ± 9 mg GAE/g in PE (27.6-fold, $p < 0.0001$). TFC rose from below quantification to 218 ± 3 mg CTE/g, Condensed tannins from 19 ± 2 to 367 ± 50 mg CTE/g ($p < 0.0001$). This enhancement is probably due to the selective adsorption of polyphenols on the hydrophobic Amberlite XAD-16 resin (Zadeh & Zeppa, 2022). Polyphenols contain aromatic rings and hydroxyl groups that enable hydrophobic and π–π interactions with the styrene–divinylbenzene matrix. On the other hand, adsorption efficiency depends on molecular polarity, molecular dimensions, and the degree of glycosylation of individual compounds. Consequently, non-phenolic polar impurities are removed, and phenolic compounds are concentrated during elution, leading to a significant increase in phenolic compounds.

Table 3
Chemical composition and antioxidant activity of crude and purified extracts of Red Prince apple peels obtained under optimal conditions (OPT, as defined in Table 1).

Analysis	Crude Extract	Purified Extract	*P*-value
Chemical composition			
Total phenolic content (mg GAE/g)	10±1	276±9	<0.0001
Total flavonoids (mg CTE/g)	<LOQ	218±3	N.A.
Condensed tannins (mg CTE/g)	19±2	367±50	<0.0001
Total anthocyanin content (mg CYE/g)	4.6 ± 0.1	30±2	<0.0001
Coler intensity (a. u.)	0.07±0.01	1.92±0.04	<0.0001
Red pigments (%)	32±<1	30±<1	<0.0001
Gallic Acid (mg/g)	<LOQ	<LOQ	N.A.
(+)-Catechin (mg/g)	<LOQ	<LOQ	N.A.
Chlorogenic acid (mg/g)	<LOQ	<LOQ	N.A.
Cyanidin-3-galactoside (mg/g)	<LOQ	4.27±0.44	N.A.
Procyanidin B2 (mg/g)	<LOQ	9.6 ± 1.6	N.A.
(-)-Epicatechin (mg/g)	0.72 ±<0.01	8.5 ± 1.5	0.018
Ferulic acid (mg/g)	<LOQ	<LOQ	NA
Hyperoside (mg/g)	1.31±0.01	16.65±2.96	0.0022
Phloridzin (mg/g)	0.34±0.04	4.72±0.54	0.0006
Chemical antioxidant capacity			
Hydroxyl radical scavenging activity (mg GAE/g)	0.15±0.01	28±<1	<0.0001
Cupric ion reducing antioxidant capacity (mg AAE/g)	22±1	1358±30	<0.0001

Note: *p*-Values were calculated using an unpaired Student *t*-test. LOQ: Limit of quantification. N.A.: Not applicable.

TAC increased from 4.6 ± 0.1 to 30 ± 2 mg CYE/g ($p < 0.0001$). Although anthocyanins are relatively polar compounds because of their glycosylated structure and the positively charged flavylium cation, they still contain conjugated aromatic systems capable of participating in hydrophobic and π–π interactions with the resin surface (Enaru et al.,

2021). Furthermore, the pore diameter of XAD-16 is also suitable for the adsorption of anthocyanins and other medium-molecular-weight phenolics (Diemer et al., 2026). Nevertheless, their lower recovery relative to other phenolic classes suggests weaker affinity for the hydrophobic matrix and incomplete desorption.

Color intensity increased from 0.07 ± 0.01 to 1.92 ± 0.04 a.u. ($p < 0.0001$). This indicates substantial enrichment of colored pigments, particularly anthocyanins, while the relative proportion of red pigments remained similar between CE and PE. This suggests that purification increased pigment concentration without significantly changing anthocyanin composition or color balance.

HPLC analysis confirmed enrichment of individual phenolics, with flavonols and flavan-3-ols predominating. Hyperoside was the most abundant compound (16.65 ± 2.96 mg/g), representing a 12.7-fold increase compared with CE. Hyperoside possesses the characteristic flavonoid C_6–C_3–C_6 structure, consisting of two aromatic rings linked by a heterocyclic C ring. These aromatic structures promote π–π interactions with the aromatic resin matrix, contributing to its adsorption and enrichment (Savic et al., 2026). Despite the presence of a galactoside fraction, hyperoside retains sufficient hydrophobicity to enable efficient adsorption onto Amberlite® XAD-16. Procyanidin B2 (9.59 ± 1.58 mg/g) and (–)-epicatechin (8.50 ± 1.49 mg/g) were also substantially enriched following purification. Chlorogenic acid remained below the quantification limit in both extracts, which may reflect its lower abundance in AP compared with pulp and flesh, and the pronounced cultivar-dependent variability reported for this compound, with some varieties exhibiting negligible or undetectable peel concentrations (Awad et al., 2000; Karaman et al., 2013). Cyanidin-3-galactoside was detected exclusively in the purified fraction (4.27 ± 0.44 mg/g), indicating selective retention of these compounds during adsorption-elution. The results align with previous data obtained for an apple cultivar from the Marche region of Italy, where procyanidins, catechins, epicatechin, flavonols, and chlorogenic acid were the predominant peel components (Giomaro et al., 2014). Overall, the magnitude of enrichment achieved in the present study highlights the effectiveness of combining UAE with resin-based purification to generate a phenolic-rich ingredient from apple processing by-products. Importantly, the purification process enhanced the concentration of existing phenolic compounds rather than altering their qualitative profile, a distinction that is critical when interpreting subsequent bioactivity results.

3.4. Evaluating the impact of partial purification on the antioxidant capacity

The impact of partial purification on the antioxidant capacity of Red Prince AP extracts was evaluated using chemical-based assays targeting distinct antioxidant mechanisms (Table 3). CUPRAC values increased from 22 to 1358 mg AAE/g dry weight, and the hydroxyl radical scavenging activity from 0.15 to 28 mg GAE/g dry weight. Similar improvements in antioxidant capacity have been observed after purifying an apple pomace extract using XAD7HP and FPX66 resins (Gonelimali et al., 2023). The antioxidant activity of AP is primarily attributed to its phenolic compounds (Kumari et al., 2023). AP typically contains the highest concentration of phenolic compounds compared to the flesh or pulp. A strong correlation exists between the TPC of AP and their antioxidant activity, with apple varieties containing higher levels of phenolics generally exhibiting greater antioxidant activity.

To further evaluate the effect of purification, its influence on copper-induced oxidation in human plasma was examined. Polyunsaturated fatty acids (PUFAs) present in plasma lipoproteins are highly susceptible to oxidative attack due to their multiple double bonds, making lipid peroxidation a primary target of reactive oxygen species (Ezekiel, 2021). The copper-induced oxidation assay revealed a clear dose-dependent response for both CE and PE at concentrations of 30 and 60 mg/L. According to Table 4, PE demonstrated greater antioxidant capacity than the CE, particularly at 30 mg/L, with values of 83 ± 10 and 49 ± 5 mg AAE/100 g, respectively. The data do not show a positive dose-dependent increase in antioxidant capacity. This lack of a positive dose-response may be associated with complex interactions between phenolic compounds and copper ions under in vitro conditions. Previous studies have reported that some antioxidants can exhibit pro-oxidant activity in the presence of transition metals such as copper. However, the present results do not directly demonstrate this mechanism (Tasaki-Handa, 2021).

Analysis of conjugated diene formation further confirmed these results (Fig. 3). Lower slope values indicate slower lipid oxidation rates and therefore stronger antioxidant activity. PE at 60 mg/L showed the lowest slope ($1.134 \times 10^{-4} \pm 1.459 \times 10^{-5}$) and the highest inhibition rate (82 ± 2%), indicating the strongest protective effect against lipid oxidation under the experimental conditions. However, the differences among treatments were not statistically significant ($p > 0.05$). CE showed similar slopes and inhibition rates at both concentrations, suggesting no dose-dependent response. The lack of a dose-dependent decrease in lipoperoxidation rate for the CE suggests that maximal antioxidant protection may have been achieved at 30 mg/L, with no additional inhibitory effect observed at the higher concentration. Additionally, potential interactions among extract constituents, including opposing antioxidant and pro-oxidant effects, may have contributed to the absence of a concentration-dependent response. Therefore, purification enhances the extract's ability to delay copper-induced lipid peroxidation, as evidenced by consistently lower oxidation rates and higher inhibition percentages in PE than in CE. The pronounced oxidation observed in the positive control (slope = 5.124×10^{-4}) confirmed the effectiveness of Cu^{2+} ions in initiating lipid peroxidation, and all extracts outperformed ascorbic acid. This protective effect is likely related to the high anthocyanin content and other phenolic compounds in the Red Prince AP extract, which is known for its strong antioxidant activity (Hassimotto et al., 2005).

3.5. Evaluation of antioxidant activity and antihemolytic effects in human erythrocytes

Since plasma lipid oxidation primarily targets PUFA-rich lipoproteins, similar oxidative mechanisms are expected in cellular membranes that are likewise enriched in polyunsaturated lipids. Erythrocytes, therefore, represent a physiologically relevant model to evaluate further the protective effects of the extracts against radical-induced damage

Table 4
The effect of crude and purified Red Prince apple peel extracts on copper-induced oxidation in human plasma.

Sample	Concentration (mg/L)	Antioxidant capacity (mg AAE/100 g)	Lipoperoxidation rate ($Abs_{245\ nm}$/min)	Inhibition rate (%)
Crude Extract	30	49 ± 5^{b}	$(2.196\times10^{-4}) \pm (6.751\times10^{-5})^{b}$	66 ± 10^{ab}
	60	37 ± 5^{c}	$(2.223\times10^{-4}) \pm (3.101\times10^{-5})^{b}$	66 ± 5^{ab}
Purified Extract	30	83 ± 10^{a}	$(1.749\times10^{-4}) \pm (4.722\times10^{-5})^{b}$	73 ± 7^{a}
	60	54 ± 4^{b}	$(1.134\times10^{-4}) \pm (1.459\times10^{-5})^{bc}$	82 ± 2^{a}
Positive Control	-	NA	$(5.124\times10^{-4}) \pm (1.196\times10^{-5})^{a}$	NA

Note: Different superscript letters within the same column indicate significant differences ($p < 0.05$) among samples, as determined by one-way ANOVA followed by Tukey test. Values sharing at least one letter are not significantly different; AAE = ascorbic acid equivalent, Positive Control = PBS without apple peel extract;. NA = not applicable.

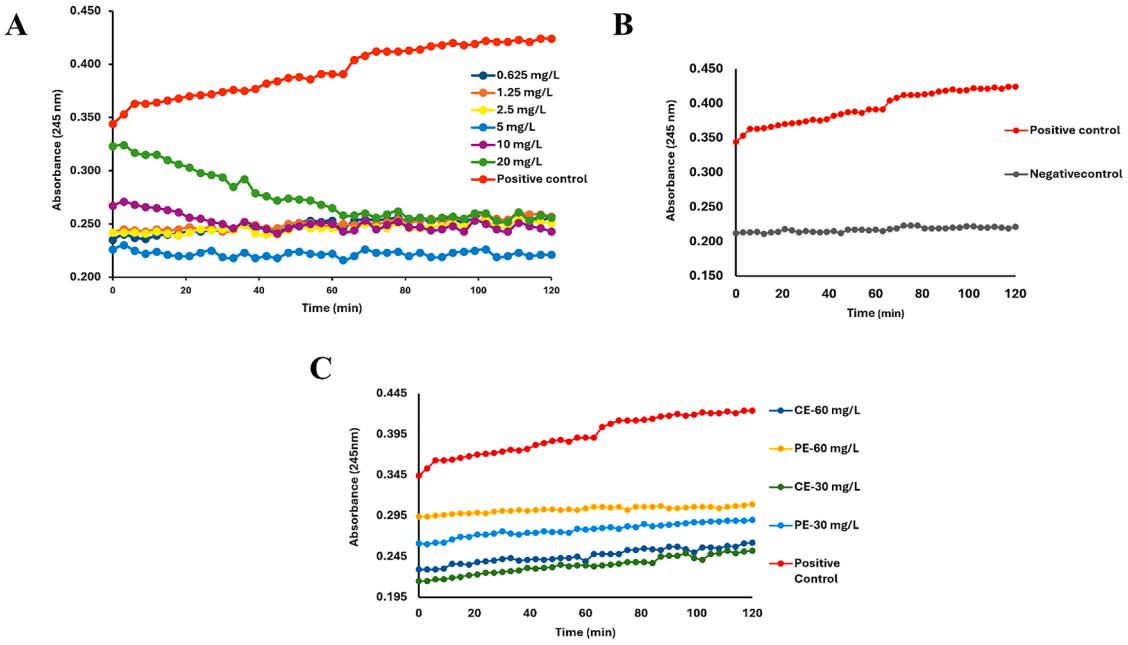

Fig. 3. Copper-induced oxidation assay in human plasma. (A) Effect of ascorbic acid concentrations (0.625 to 20 mg/L) on plasma oxidation; (B) Validation of the assay using positive and negative controls (PC and NC, respectively); (C) Effects of crude (CE) and purified (PE) Red Prince apple peel extracts on conjugated diene formation in human plasma compared with the PC representing maximum oxidation. Note: Quantitative data are presented as mean ± standard deviation (n = 4).

(Mariano et al., 2022). The protective effects of different concentrations of CE and PE (selected based on their TPC values) against oxidative damage in human erythrocytes were evaluated using AAPH-induced hemolysis and intracellular ROS generation as complementary

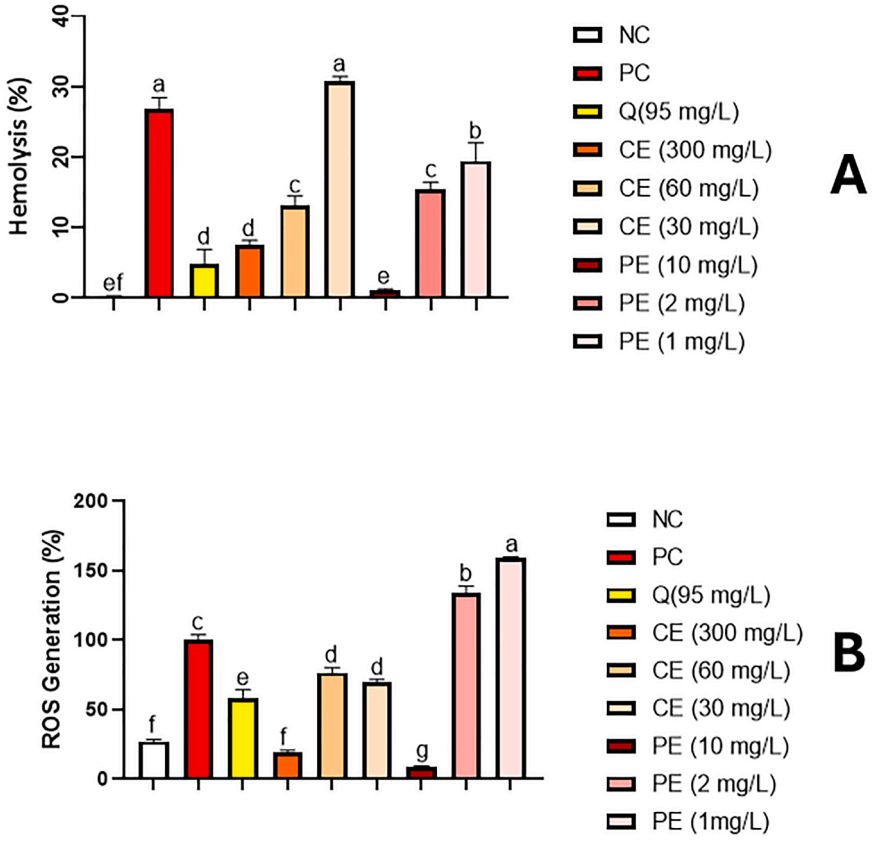

Fig. 4. Effects of crude (CE) and purified (PE) from Red Prince apple peel at concentrations of 1, 2, 10, 30, 60, and 300 mg/L on human red blood cells. (A) Inhibition of hemolysis and (B) reduction of intracellular reactive oxygen species (ROS) generation induced by AAPH-derived peroxyl radicals. Data are compared to the negative control (NC), the positive control (PC), and quercetin (Q). Note: Quantitative data are presented as mean ± standard deviation (n = 4). Different letters comparing treatments represent statistically different means ($p < 0.05$).

endpoints (Fig. 4A, B). Exposure of erythrocytes to AAPH increased the hemolysis rate and intracellular ROS accumulation relative to the negative control (i.e., no AAPH addition), reflecting sustained peroxyl radical generation and oxidative injury. Both CE (30–300 mg/L) and PE (1–10 mg/L) significantly reduced erythrocyte hemolysis in a concentration-dependent manner ($p < 0.05$), with PE exhibiting markedly stronger protective effects than CE. The highest protective activity was observed at 300 mg/L CE and 10 mg/L PE, resulting in average hemolysis percentages of 7.5% and 1.2%, respectively. Notably, PE at 10 mg/L exhibited stronger antihemolytic activity than quercetin, which showed an average hemolysis of 3.6%, whereas the positive control showed substantially higher hemolysis (26.8%).

The observed protective effects can be partially attributed to the physicochemical properties of AP's polyphenols. Due to their predominantly hydrophilic nature, these compounds are unlikely to penetrate the hydrophobic core of the erythrocyte membrane (Cyboran-Mikołajczyk et al., 2022). Instead, they associate with the outer monolayer, interacting with the polar head groups of membrane lipids. This surface binding enhances membrane stability, as reflected by the increased resistance of erythrocytes to osmotic stress. Therefore, it is hypothesized that the extract components can effectively scavenge free radicals in the surrounding aqueous phase. They form a protective barrier that limits radical access to the membrane, consequently reducing lipid peroxidation. These findings are consistent with a previous study on extract obtained from Redfield apple flesh using ethanol (0.05 g/mL), which has been reported to delay red blood cell hemolysis, highlighting the protective role of apple polyphenols against oxidative membrane damage (Kondo et al., 2007). Another study has shown that apple polyphenol extracts do not induce hemolysis within the concentration range of 0.1–0.5 mg/mL, confirming their non-hemolytic and biocompatible nature (Cyboran et al., 2012). Furthermore, methanolic extracts from Maharaji AP have been demonstrated to effectively inhibit H_2O_2-induced hemolysis in erythrocytes (Ahmad et al., 2023). Although a different oxidative system was employed, both AAPH and H_2O_2 generate reactive oxygen species that compromise erythrocyte membrane integrity.

Red blood cells play a vital role in preserving redox balance in the blood (Gwozdzinski et al., 2021). When this balance is disturbed, oxidative stress can develop, often due to an excess of ROS or a weakened antioxidant defense system. Intracellular ROS measurements further supported PE's (10 mg/L) superior antioxidant performance compared to CE (300 mg/L). The optimal concentrations of CE (300 mg/L) and PE (10 mg/L) significantly reduced AAPH-induced intracellular ROS generation (Fig. 4B). At these concentrations, CE and PE decreased ROS levels by 19% and 9%, respectively, compared with the PC, indicating modest cellular antioxidant activity. Lower PE concentrations (1 and 2 mg/L) failed to provide adequate antioxidant protection, suggesting a potential pro-oxidant effect compared to the PC (Tedesco et al., 2021). Cellular antioxidant effect is likely linked to the phenolic compounds present in the apple peel extracts, which can stabilize red blood cell membranes and inhibit hemoglobin polymerization (Mpiana et al., 2010). The present study is consistent with prior findings that apple, strawberry, and chokeberry extracts protect against lipid oxidation in red blood cell membranes induced by the AAPH radical (Bonarska-Kujawa et al., 2012). Apple extract exhibited the strongest effect, providing up to 100% protection at concentration of 0.05 mg/mL. Similarly, Perrone et al. reported that $HgCl_2$ exposure increased intracellular ROS levels by approximately threefold compared with the control. Among the different Annurca apple extracts (concentrations 1–5 μM), the ripe peel extract exhibited the strongest antioxidant activity in a dose-dependent manner. At the highest tested concentration (5 μM), the ripe peel extract almost completely restored ROS levels to those of the untreated control, whereas the ripe flesh, unripe peel, and unripe flesh extracts also reduced ROS but to a lesser extent (Perrone et al., 2025). The differences in ROS reduction across studies likely reflect variations in oxidative stress models, with $HgCl_2$ representing a more severe pro-oxidant challenge than AAPH, as well as differences in phenolic content among apple varieties.

3.6. Cytotoxic and cellular antioxidant activity of CE and PE in monoculture and 3D spheroid

Cytotoxic and antioxidant potential of CE and PE at various concentrations (5–300 μg/mL) was evaluated using HepG2 cells. HepG2 cells are known to express phase I and phase II enzymes involved in the metabolism of drugs and various xenobiotic compounds. Therefore, they are a suitable in vitro model for screening the safety of the extracts investigated in this study (Valentin-Severin et al., 2003).

The results in Fig. 5A indicate that CE (5–300 μg/mL) did not exhibit cytotoxicity in the HepG2 cell line after 24 h of treatment. In contrast, the PE reduced HepG2 cell viability to 76% at 300 μg/mL. Despite this reduction in cell viability, it was not possible to determine the IC_{50} value for this cell line. Therefore, under the tested conditions, both extracts are weakly cytotoxic, with IC_{50} values greater than 300 μg/mL (Goldin et al., 1981). Data reported by Faramarzi et al. (2015) demonstrated that AP extracts of the 'Bekran' and 'Bastam' apple varieties obtained by UAE and CH_3OH/HCOOH solution (19:1, v/v), at the concentrations (15.62, 31.25, 62.50, 125.0, and 250.0 μg/mL), did not exert adverse effects on the viability of human epithelial (HeLa) and hepatic (HepG2) cells after 24, 48, and 72 h of incubation. In another study, the cytotoxic and antiproliferative activities of AP extract obtained with 80% acetone were evaluated in HepG2 cells (Xia et al., 2024). The reported IC_{50} value of 150 mg/mL indicates that the antiproliferative effect occurs at concentrations at which the AP extract remains non-toxic.

Regarding cellular antioxidant activity, both CE and PE reduced AAPH-induced ROS generation in HepG2 cells after 24 h of treatment (Fig. 5B). For CE, ROS production decreased in a concentration-dependent manner, with the greatest reduction observed at 50 μg/mL (approximately 74% of the PC). In contrast, PE elicited a more modest response, with ROS levels ranging from approximately 75–87% of the PC across the tested concentrations (5–100 μg/mL). Although the lowest ROS production was observed at 5 μg/mL, no significant differences were detected among PE concentrations, nor did any differ significantly from the PC. These results align with a study on phlorizin extracted from apple or apple juice, which reported a protective effect of phlorizin on antioxidant stress and apoptosis in H_2O_2-induced HepG2 cells (Wang et al., 2019). The major phenolic constituents in apples include flavonols, hydroxycinnamic acids, flavan-3-ols, dihydrochalcones, and anthocyanins, which are known for their significant antioxidant properties (Liang et al., 2020; Shoji et al., 2004). The content and distribution of these phenolic compounds vary across tissue types, demonstrating clear tissue specificity (Dhyani et al., 2018). Furthermore, Liang et al. (2020) reported that the TPC and total proanthocyanidin contents are significantly higher in the peel than in the pulp.

Three-dimensional (3D) culture models are widely recognized for offering several advantages over traditional two-dimensional (2D) monolayer cultures, as they more accurately mimic the in vivo tumor microenvironment. Given that both CE and PE exhibited weak cytotoxicity in monoculture, with IC_{50} values greater than 300 μg/mL, their cytotoxic activity and effects on cell viability were further evaluated using HepG2 cellular spheroids (a 3D culture model). The spheroids were treated with extract concentrations of 100, 200, and 300 μg/mL for 72 h. In addition, this study assessed whether CE and PE could alter the volume, morphology, and structural integrity of HepG2 spheroids (Fig. 5C).

According to the results, the viability of HepG2 spheroids treated with both CE and PE remained largely unchanged. A reduction in cell viability of approximately 91% was observed only at 300 μg/mL in spheroids treated with PE. Therefore, overall, no significant cytotoxic effect was detected for the tested treatments. Regarding the morphometric parameters of the 3D cultures, changes in spheroid area and diameter were observed in HepG2 spheroids treated with CE only at 24,

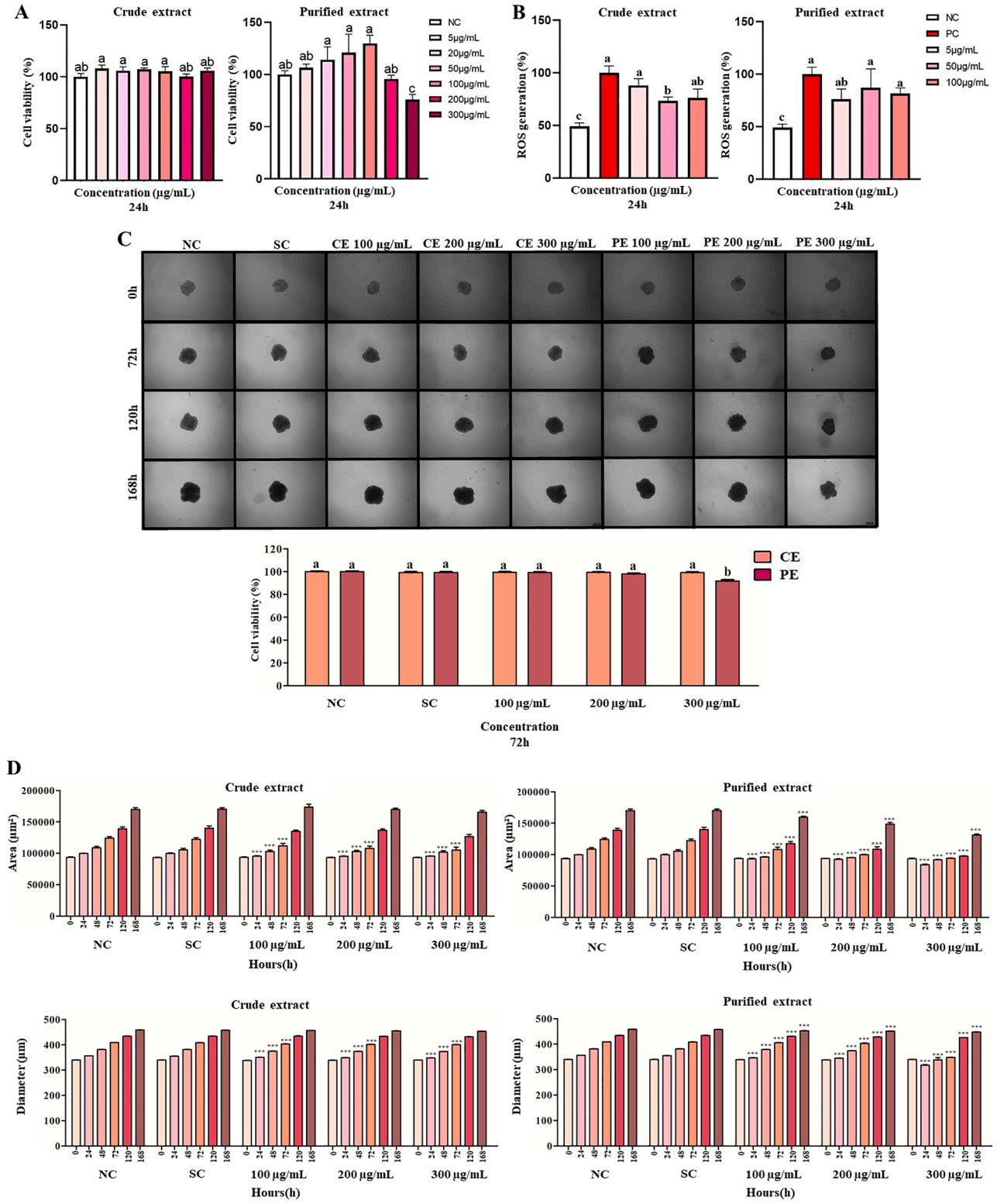

Fig. 5. Effects of crude (CE) and purified (PE) Red Prince apple peel extracts on HepG2 cells and spheroids. (A) Cell viability determined by the MTT assay following 24 h exposure to CE and PE (5–300 µg/mL). (B) Intracellular reactive oxygen species (ROS) production in HepG2 monolayer cultures after 24 h treatment with CE and PE at 5, 50, and 100 µg/mL. (C) Effects of CE and PE on HepG2 spheroid viability, morphology, structural integrity, area (µm²), and diameter (µm) evaluated at 0 h (Day 4), 24 h (Day 5), 48 h (Day 6), 72 h (Day 7), 120 h (Day 9), and 168 h (Day 11). Images were acquired using an Axio Cam MRc camera coupled to an Axio Lab.A1 microscope equipped with a 4× objective lens. Values are presented as mean ± standard deviation. Means sharing the same letter are not significantly different ($p > 0.05$), whereas different letters indicate significant differences among treatments ($p < 0.05$). NC, negative control (culture medium); SC, solvent control (0.5% v/v DMSO). Scale bar = 200 µm.

48, and 72 h (Fig. 5C). In contrast, spheroids treated with PE showed alterations in these parameters at all evaluated time points (24, 48, 72, 120, and 168 h). Concerning 3D cell culture models, no studies were found in the literature reporting the treatment of cellular spheroids with Red Prince AP. Therefore, the treatment evaluated in the present study can be considered novel.

3.7. In vitro anti-obesity evaluation by enzymatic inhibition

The potential of CE and PE to modulate obesity-related metabolic targets was evaluated through dose-dependent in vitro inhibition assays of pancreatic lipase and HMG-CoA reductase (Table 5). Both extracts demonstrated dose-dependent activity, with PE ($IC_{50} = 45.74 \pm 0.99$ μg/mL) exhibiting stronger lipase inhibition than CE ($IC_{50} = 56.55 \pm 5.21$ μg/mL) ($p < 0.05$). However, AP extracts were less effective than the standard drug Orlistat (37.38±2.42). These findings align with previous reports demonstrating dose-dependent lipase inhibition by apple polyphenols, particularly the procyanidin fraction found in both CE and PE, which exhibits enhanced potency ($IC_{50} = 1.4–5.6$ μg/mL) and is recognized as a key contributor to enzyme inhibition (Sugiyama et al., 2007). Similarly, both extracts showed comparable inhibitory activity against HMGCR, with IC_{50} values of 42.80 ± 1.25 μg/mL for CE and 40.98 ± 1.86 μg/mL for PE. PE exhibited a significantly lower IC_{50} than CE ($p < 0.05$), indicating slightly greater inhibitory potency. However, both were less effective than simvastatin ($IC_{50} = 33.04 \pm 2.70$ μg/mL).

While direct in vitro studies on apple-derived extracts are limited, in comparison, phenolic extracts from thinned apples evaluated against pravastatin showed higher IC_{50} values. The most active cultivar, Verde Doncella, showed an IC_{50} of 100.88 ± 3.93 μg/mL (Cano-Lou et al., 2026). Although different reference statins were used, these comparisons suggest that CE and PE exhibit relatively stronger HMGCR inhibitory activity than previously reported apple phenolics. These results highlight the potential of CE and PE as hypocholesterolaemic agents, with the stronger activity observed in PE. This may be attributed to the concentration of bioactive constituents during purification (Kim et al., 2023), especially anthocyanins and other flavonoids (Oteiza et al., 2018).

HMG-CoA reductase serves as the rate-limiting enzyme of the mevalonate pathway and plays a central role in endogenous cholesterol biosynthesis (Iqbal et al., 2014). Although inhibition of this enzyme alone does not constitute direct evidence of anti-obesity activity, dysregulation of cholesterol and lipid metabolism is closely associated with obesity and related metabolic disorders. Inhibition of HMGCR suppresses mevalonate formation, thereby reducing cholesterol synthesis and the production of very low-density and low-density lipoproteins (Tjandrawinata et al., 2026). Furthermore, modulation of the mevalonate pathway has been associated with improved adiponectin regulation, reduced oxidative stress and inflammation, and enhanced lipid homeostasis. Therefore, evaluating HMGCR alongside pancreatic lipase provides complementary information about the extracts' ability to influence both dietary lipid digestion and endogenous lipid metabolism (Kim et al., 2023; Oteiza et al., 2018).

Table 5
IC_{50} values of crude and purified Red Prince apple peel extracts against porcine pancreatic lipase and HMGCR (3-hydroxy-3-methylglutaryl-CoA reductase) enzymes.

Assay	Sample	IC_{50} (μg/mL)
Lipase	Orlistat	37.4 ± 2.4 [c]
	Crude Extract	56.5 ± 5.2 [a]
	Purified Extract	45.7 ± 1.0 [b]
HMGCR	Simvastatin	33.0 ± 2.7 [c]
	Crude Extract	42.8 ± 1.2 [a]
	Purified Extract	41.0 ± 1.9 [b]

Note: Different letters in the same column when comparing the controls (e.g., orlistat and simvastatin) and Red Princess apple peel extracts for the same assay indicate statistically different means ($p < 0.05$).

4. Conclusions

In this study, response surface methodology identified the optimal ultrasound-assisted extraction conditions as a solid-to-solvent ratio of 1:50, ultrasound power of 500 W, and ethanol concentration of 50%. Subsequent purification using Amberlite® XAD-16 macroporous resin substantially enhanced the phytochemical profile of AP extracts by concentrating TPC, TFC, TAC, and condensed tannins. Hyperoside, procyanidin B2, and epicatechin were identified as the predominant phenolic compounds in the purified extract (PE). The partial reversibility of anthocyanins (80.4%) further indicated their relative stability under the evaluated processing conditions and supports the potential incorporation of the purified extract into acidic food formulations. The erythrocyte model demonstrated that both extracts exert membrane-protective effects against AAPH-induced oxidative stress. These results further support the biological potential of phenolic compounds, particularly those enriched in AP. Both CE and PE exhibit a favorable safety profile, showing weak cytotoxicity toward HepG2 cells in both 2D and 3D culture models ($IC_{50} > 300$ μg/mL). In addition, both extracts reduced AAPH-induced intracellular ROS generation, with CE displaying a more pronounced antioxidant effect than PE. In addition, both extracts demonstrated a dose-dependent inhibition of pancreatic lipase and HMG-CoA reductase, indicating their potential to modulate obesity-related metabolic targets. These findings highlight the effectiveness of macroporous resin purification in enhancing both the antioxidant activity and inhibitory effects on obesity-related metabolic targets. The results also support the potential application of these extracts as functional bioactive ingredients in food systems. Moreover, the purification process demonstrated technological potential to convert AP, an abundant agro-industrial by-product, into a concentrated, phenolic-rich ingredient. The high adsorption capacity, selectivity, chemical stability, and potential reusability of macroporous resins provide advantages for developing scalable purification processes for food applications.

Further research should focus on validating and scaling up the optimized extraction process at pilot and industrial scales, as well as on developing and formulating food-grade extracts. Mechanistic studies, adipocyte-based investigations, and in vivo evaluations are also needed to validate their potential in obesity management and support their application as functional food ingredients within a circular bioeconomy framework.

5. Ethics statement

The protocol involving human blood collection was reviewed and approved by the University of Limerick Science and Engineering Research Ethics Committee (approval numbers 2023_02_01_S&E and 2025_05_07_S&E). The participant provided written informed consent prior to blood collection, in accordance with institutional ethical guidelines and the principles of the Declaration of Helsinki.

CRediT authorship contribution statement

Nikoo Ostovar: Writing – original draft, Investigation, Formal analysis, Data curation. **Carolina Girotto Pressete:** Writing – original draft, Visualization, Methodology, Investigation, Formal analysis. **Fahrul Nurkolis:** Writing – review & editing, Visualization, Methodology, Investigation, Data curation. **Lusânia Maria GreggiAntunes:** Writing – review & editing, Resources, Methodology, Funding acquisition. **Fabiana Andrea Hoffmann Sarda:** Writing – review & editing, Supervision, Methodology. **George Barreto:** Writing – review & editing, Supervision, Methodology. **Daniel Granato:** Writing – review & editing, Supervision, Software, Resources, Project administration, Methodology, Funding acquisition, Data curation, Conceptualization.

Declaration of competing interest

The authors declare that they have no known competing financial interests or personal relationships that could have appeared to influence the work reported in this paper.

Acknowledgements

The authors are grateful to Research Ireland (grant No 22/FFP-P/11380) for funding this work. The authors also acknowledge Dr Con Traas (The Apple Farm, Ireland) for providing the agro-industrial side streams of Red Prince apple peels used in the study. The graphical abstract was created by the authors using schematic design and icons obtained from Flaticon, Illustrae, and the BioRender app, which were combined in Microsoft PowerPoint 365. The final figure was entirely designed, assembled, and validated by the authors. The authors confirm that the figure represents the data provided in the manuscript. During the preparation of this work, Grammarly Pro was used to correct the text's syntax, grammar, and readability, without generating content. After using this tool, the authors reviewed and edited the text as needed and take full responsibility for the content of the published article.

Supplementary materials

Supplementary material associated with this article can be found, in the online version, at doi:10.1016/j.afres.2026.102456.

Data availability

Data will be made available on request.

References

Ahmad, A., Amit, S., Rawat, A., Parihar, T., & Pandey, N. (2023). Relative phenolic profile, ROS scavenging, and anti-haemolytic potential of polarity-driven peel bioactive compounds of distinct malus species indigenous to Kashmir. *Journal of Medical Pharmaceutical and Allied Sciences, 12*(4), 5911–5920. https://doi.org/10.55522/jmpas.V12I4.4400

Awad, M. A., de Jager, A., & van Westing, L. M. (2000). Flavonoid and chlorogenic acid levels in apple fruit: Characterisation of variation. *Scientia Horticulturae, 83*(3–4), 249–263. https://doi.org/10.1016/S0304-4238(99)00124-7

Apak, R. (2018). Electron transfer-based antioxidant capacity assays and the cupric ion reducing antioxidant capacity (CUPRAC) assay.In Measurement of Antioxidant Activity & Capacity (eds R. Apak, E. Capanoglu and F. Shahidi). https://doi.org/10.1002/9781119135388.ch4.

Bal-Price, A., & Coecke, S. (2011). Guidance on good cell culture practice (GCCP). *Neuromethods, 56*, 1–25. https://doi.org/10.1007/978-1-61779-077-5_1

Bonarska-Kujawa, D., Sarapuk, J., Bielecki, K., Oszmiański, J., & Kleszczyńska, H. (2012). Antioxidant activity of extracts from apple, chokeberry and strawberry. *Polish Journal of Food and Nutrition Sciences, 62*(4), 229–234. https://doi.org/10.2478/v10222-012-0055-7

Cano-Lou, J., Casado-Hidalgo, G., Les, F., Pina, A., Acquaticci, L., Caprioli, G., & López, V. (2026). Phenolic compounds and multifunctional properties of thinned apples: Revalorizing fruit by-products for industrial applications. *Food Chemistry: X, 34*, Article 103640. https://doi.org/10.1016/j.fochx.2026.103640

Cyboran, S., Oszmiański, J., & Kleszczyńska, H. (2012). Interaction between plant polyphenols and the erythrocyte membrane. *Cellular and Molecular Biology Letters, 17*(1), 77–88. https://doi.org/10.2478/s11658-011-0038-4

Cyboran-Mikołajczyk, S., Męczarska, K., Solarska-Ściuk, K., Ratajczak-Wielgomas, K., Oszmiański, J., Jencova, V., & Bonarska-Kujawa, D. (2022). Protection of erythrocytes and microvascular endothelial cells against oxidative damage by Fragaria vesca L. and Rubus idaeus L. leaves extracts—The mechanism of action. *Molecules, 27*(18), 5865. https://doi.org/10.3390/molecules27185865

Dai, K., Wei, Y., Jiang, S., Xu, F., Wang, H., Zhang, X., & Shao, X. (2022). Lab scale extracted conditions of polyphenols from thinned peach fruit have antioxidant, hypoglycemic, and hypolipidemic properties. *Foods, 11*(1), 99. https://doi.org/10.3390/foods11010099

Dhyani, P., Bahukhandi, A., Rawat, S., Bhatt, I. D., & Rawal, R. S. (2018). Diversity of bioactive compounds and antioxidant activity in Delicious group of apple in Western Himalaya. *Journal of Food Science and Technology, 55*, 2587–2599. https://doi.org/10.1007/s13197-018-3179-x

Diemer, E., Lemaire, J., Scrive, M., Nabil, G., & Morad, C. (2026). Purification of caffeoylquinic acids from forced chicory roots using macroporous resins: Experimental investigation and advanced modeling of adsorption kinetics and equilibria. *ACS Sustainable Chemistry and Engineering, 14*(1), 450–465. https://doi.org/10.1021/acssuschemeng.5c09784

Enaru, B., Dret, G., Pop, T. D., Stănilă, A., & Diaconeasa, Z. (2021). Anthocyanins : Factors affecting their stability and degradation. *Antioxidants, 10*(12), 1967. https://doi.org/10.3390/antiox10121967

Escher, G. B., Santos, J. S., Rosso, N. D., Marques, M. B., Azevedo, L., do Carmo, M. A. V., & Granato, D. (2018). Chemical study, antioxidant, anti-hypertensive, and cytotoxic/cytoprotective activities of Centaurea cyanus L. petals aqueous extract. *Food and Chemical Toxicology, 118*, 439–453. https://doi.org/10.1016/j.fct.2018.05.046

Ezekiel, K.O. (2021). Lipid Peroxidation and the Redox Effects of Polyherbal. In: Accenting lipid peroxidation. Editor: Pınar Atukeren. Intech Open. doi:10.5772/intechopen.97625.

Faramarzi, S., Pacifico, S., Yadollahi, A., Lettieri, A., Nocera, P., & Piccolella, S. (2015). Red-fleshed apples: Old autochthonous fruits as a novel source of anthocyanin antioxidants. *Plant Foods for Human Nutrition, 70*(3), 324–330. https://doi.org/10.1007/s11130-015-0497-2

Farrell, M., Lima, A.dos S., Mohammadi, N., Cruz, T. M., Zhou, F., Xu, Y. Q., … Granato, D. (2024). Microencapsulation of purple tea polyphenols using the vibrating nozzle ionotropic gelation technology: Metabolomics, bioactivity, and application in milky tea. *LWT - Food Science and Technology,, 199*, Article 116099. https://doi.org/10.1016/j.lwt.2024.116099

Fidelis, M., Santos, J. S., Escher, G. B., Vieira do Carmo, M., Azevedo, L., Cristina da Silva, M., & Granato, D. (2018). In vitro antioxidant and antihypertensive compounds from camu-camu (Myrciaria dubia McVaugh, Myrtaceae) seed coat: A multivariate structure-activity study. *Food and Chemical Toxicology, 120*, 479–490. https://doi.org/10.1016/j.fct.2018.07.043

Franchin, M., de Lima Xavier, B. T., Guo, Y., Luo, L., Wang, K., & Granato, D. (2025). Advancing antioxidant testing: Standardisation of a human plasma oxidation assay and its integration with chemical and cellular protocols. *Food Research International, 218*, Article 116951. https://doi.org/10.1016/j.foodres.2025.116951

Friedrich, J., Seidel, C., Ebner, R., & Kunz-Schughart, L. A. (2009). Spheroid-based drug screen: Considerations and practical approach. *Nature Protocols, 4*(3), 309–324. https://doi.org/10.1038/nprot.2008.226

Garcia, D. A., Pressete, C. G., Miranda, R., Salem, P. P. O., Nicácio, K. J., Costa, L. P. D. M., … Chagas-Paula, D. A. (2024). Biological and metabolomics-guided isolation of tetrahydrofurofuran lignan from Croton spp. with antiproliferative activity against human melanoma cell line. *Fitoterapia, 177*, Article 106070. https://doi.org/10.1016/j.fitote.2024.106070

Giomaro, G., Karioti, A., Bilia, A. R., Bucchini, A., Giamperi, L., Ricci, D., & Fraternale, D. (2014). Polyphenols profile and antioxidant activity of skin and pulp of a rare apple from Marche region (Italy). *Chemistry Central Journal, 8*, 1–10. https://doi.org/10.1186/1752-153X-8-4545.

Goldin, A., Venditti, J. M., Macdonald, J. S., Muggia, F. M., Henney, J. E., & Devita, V. T. (1981). Current results of the screening program at the division of cancer treatment, national cancer institute. *European Journal of Cancer, 17*(2), 129–142. https://doi.org/10.1016/0014-2964(81)90027-X, 1965.

Gonelimali, F., Szabó-Nótin, B., & Máté, M. (2023). Purification of the apple pomace polyphenol extract using adsorbent resin. *Progress in Agricultural Engineering Sciences, 19*, 97–104. https://doi.org/10.1556/446.2023.00087

Gong, L., Wu, Y., Qiu, X., Xin, X., An, F., & Guo, M. (2022). Adsorption characteristics and enrichment of emodin from marine-derived Aspergillus flavipes HN4-13 extract by macroporous resin XAD-16. *Marine Drugs, 20*(4), 231. https://doi.org/10.3390/md20040231

Granato, D. (2026). Peroxyl radical-induced lipid peroxidation in bovine plasma: Kinetic parameters for simultaneous antioxidant activity and capacity assessments of foods. *Food Research International, 233*, 118964. https://doi.org/10.1016/j.foodres.2026.118964

Gwozdzinski, K., Pieniazek, A., & Gwozdzinski, L. (2021). Review article reactive oxygen species and their involvement in red blood cell damage in chronic kidney disease. *Oxidative Medicine and Cellular Longevity, 2021*, 6639199. https://doi.org/10.1155/2021/6639199

Hassimotto, N. M. A., Genovese, M. I., & Lajolo, F. M. (2005). Antioxidant activity of dietary fruits, vegetables, and commercial frozen fruit pulps. *Journal of Agricultural and Food Chemistry, 53*(8), 2928–2935. https://doi.org/10.1021/jf047894h

Hiranpradith, V., Therdthai, N., Soontrunnarudrungsri, A., & Rungsuriyawiboon, O. (2025). Optimisation of ultrasound-assisted extraction of total phenolics and flavonoids content from Centella asiatica. *Foods, 14*(2), 291. https://doi.org/10.3390/foods14020291

Huaman-Castilla, N. L., Mart, M., Camilo, C., Pedreschi, F., Mariotti-celis, M., & Ricardo, P. (2019). The impact of temperature and ethanol concentration on the global recovery of specific polyphenols in an integrated HPLE/RP process on Carménère pomace extracts. *Molecules, 24*(17), 3145. https://doi.org/10.3390/molecules24173145

Iqbal, D., Khan, M. S., Khan, M. S., Ahmad, S., & Srivastava, A. K. (2014). An in vitro and molecular informatics study to evaluate the antioxidative and β-hydroxy-β-methylglutaryl-CoA reductase inhibitory property of Ficus virens Ait. *Phytotherapy Research, 28*(6), 899–908. https://doi.org/10.1002/ptr.5077

Karaman, Ş., Tütem, E., Başkan, K. S., & Apak, R. (2013). Comparison of antioxidant capacity and phenolic composition of peel and flesh of some apple varieties. *Journal of the Science of Food and Agriculture, 93*(4), 867–875. https://doi.org/10.1002/jsfa.5810

Kim, H., Jeon, Y., Kim, S., Jung, J., Ko, D., & Kim, E. (2023). Agaricus bisporus extract exerts an anti-obesity effect in high-fat diet-induced obese C57BL/6N mice by inhibiting pancreatic lipase-mediated fat absorption. *Nutrients, 15*(19), 4225. https://doi.org/10.3390/nu15194225

Kondo, S., Yoshikawa, H., & Miwa, N. (2007). Cytoprotective effect of fruit extracts associated with antioxidant activity against ultraviolet rays. *Food Chemistry, 104*(3), 1272–1276. https://doi.org/10.1016/j.foodchem.2007.01.001

Köpsel, M., Kostka, T., Niesen, S., Winterhalter, P., & Esatbeyoglu, T. (2025). Influence of fractionation of polyphenols by membrane chromatography on antioxidant, antimicrobial and proliferation-inhibiting effects of red fruit juices. *Food Chemistry, 463*, Article 141216. https://doi.org/10.1016/j.foodchem.2024.141216

Kumari, S., Manohar, S., Kumari, P., Krishnan, V., Maheshwari, C., Narwal, S., Prakash Gupta, O., T. Gowda, V., Bansal, N., & Dahuja, A. (2023). The role of major phenolics in apple to total antioxidant capacity. *Apple Cultivation - Recent Advances*, 1–18. https://doi.org/10.5772/intechopen.109064

Lee, J., Durst, R. W., & Wrolstad, R. E. (2005). Determination of total monomeric anthocyanin pigment content of fruit juices, beverages, natural colorants, and wines by the pH differential method: Collaborative study. *Journal of AOAC International, 88* (5), 1269–1278. https://doi.org/10.1093/jaoac/88.5.1269

Li, Q., Zhang, F., Wang, Z., Feng, Y., & Han, Y. (2023). Advances in the preparation, stability, metabolism, and physiological roles of anthocyanins: A review. *Foods, 12* (21), 3969. https://doi.org/10.3390/foods12213969

Liang, X., Zhu, T., Yang, S., Li, X., Song, B., Wang, Y., & Cao, J. (2020). Analysis of phenolic components and related biological activities of 35 apple (Malus pumila Mill.) cultivars. *Molecules, 25*(18), 4153. https://doi.org/10.3390/molecules25184153

Mantiniotou, M., Bujor, B. C., Athanasiadis, V., Chatzimitakos, T., Kalompatsios, D., Kotsou, K., & Lalas, S. I. (2024). Response surface methodology-aided optimization of bioactive compound extraction from apple peels through pulsed electric field pretreatment and ultrasonication. *Eng, 5*(4), 2886–2901. https://doi.org/10.3390/eng5040150

Margraf, T., Karnopp, A. R., Rosso, N. D., & Granato, D. (2015). Comparison between Folin-Ciocalteu and Prussian Blue assays to estimate the total phenolic content of juices and teas using 96-well microplates. *Journal of Food Science, 80*(11), C2397–C2403. https://doi.org/10.1111/1750-3841.13077

Mariano, A., Bigioni, I., Misiti, F., Fattorini, L., Scotto, A., & Rodio, A. (2022). The nutraceuticals as modern key to achieve erythrocyte oxidative stress fighting in osteoarthritis. *Current Issues in Molecular Biology, 44*(8), 3481–3495. https://doi.org/10.3390/cimb44080240

Mohammadi, N., Franchin, M., Girotto Pressete, C., Maria Greggi Antunes, L., & Granato, D. (2024a). Green recovery and application of berry anthocyanins in functional gummies: Stability study, plasma and cellular antioxidant and anti-inflammatory activity. *Food Research International, 196*, Article 115128. https://doi.org/10.1016/j.foodres.2024.115128

Mohammadi, N., Guo, Y., Wang, K., & Granato, D. (2024b). Macroporous resin purification of phenolics from Irish apple pomace: Chemical characterization, and cellular antioxidant and anti-inflammatory activities. *Food Chemistry, 437*(P1), Article 137815. https://doi.org/10.1016/j.foodchem.2023.137815

Mpiana, P. T., Ngbolua, K. N. N., Bokota, M. T., Kasonga, T. K., Atibu, E. K., Tshibangu, D. S. T., & Mudogo, V. (2010). In vitro effects of anthocyanin extracts from Justicia secunda Vahl on the solubility of haemoglobin S and membrane stability of sickle erythrocytes. *Blood Transfusion, 8*, 248–254. https://doi.org/10.2450/2009.0120-09

Nayebhashemi, M., Enayati, S., Zahmatkesh, M., Madanchi, H., Saberi, S., Mostafavi, E., … Khalaj, V. (2023). Surface display of pancreatic lipase inhibitor peptides by engineered Saccharomyces boulardii: Potential as an anti-obesity probiotic. *Journal of Functional Foods, 102*, Article 105458. https://doi.org/10.1016/j.jff.2023.105458

Oteiza, P. I., Fraga, C. G., Mills, D. A., & Taft, D. H. (2018). Flavonoids and the gastrointestinal tract: Local and systemic effects. *Molecular Aspects of Medicine, 61*, 41–49. https://doi.org/10.1016/j.mam.2018.01.001

Pap, N., Reshamwala, D., Korpinen, R., Kilpeläinen, P., Fidelis, M., Furtado, M. M., Sant'Ana, A. S., Wen, M., Zhang, L., Hellström, J., Marnilla, P., Mattila, P., Sarjala, T., Yang, B., Lima, A.dos S., Azevedo, L., Marjomäki, V., & Granato, D. (2021). Toxicological and bioactivity evaluation of blackcurrant press cake, sea buckthorn leaves and bark from Scots pine and Norway spruce extracts under a green integrated approach. *Food and Chemical Toxicology, 153*, Article 11228. https://doi.org/10.1016/j.fct.2021.112284

Park, N. Y., Cho, S. D., Chang, M. S., & Kim, G. H. (2022). Optimization of the ultrasound-assisted extraction of flavonoids and the antioxidant activity of Ruby S apple peel using the response surface method. *Food Science and Biotechnology, 31*, 1667–1678. https://doi.org/10.1007/s10068-022-01150-8

Perrone, P., Moriello, C., Alessio, N., Manna, C., & D'Angelo, S. (2025). Cytoprotective potential of annurca apple polyphenols on mercury-induced oxidative stress in Human erythrocytes. *International Journal of Molecular Sciences, 26*(18), 8826. https://doi.org/10.3390/ijms26188826

Prieto, A. M., dos Santos, A. G., Oliveira, A. P. S., Cavalheiro, A. J., Silva, D. H. S., Bolzani, V. S., … Soares, C. P. (2013). Assessment of the chemopreventive effect of casearin B, a clerodane diterpene extracted from Casearia sylvestris (Salicaceae). *Food and Chemical Toxicology, 53*, 153–159. https://doi.org/10.1016/j.fct.2012.11.029

Ramírez-Moreno, E., Arias-Rico, J., Jiménez-Sánchez, R. C., Estrada-Luna, D., Jiménez-Osorio, A. S., Zafra-Rojas, Q. Y., … Sandoval-Gallegos, E. M. (2022). Role of bioactive compounds in obesity: Metabolic mechanism focused on inflammation. *Foods, 11*(9), 1232. https://doi.org/10.3390/foods11091232

Riaz, A., Yousaf, K., Abdin, M., Jabbar, S., Abid, M., & Hashim, M. M. (2020). Extraction optimization, purification and immunostimulatory activity in vitro of polyphenols from apple (Malus domestica) peel. *Sains Malaysiana, 49*(7), 1553–1566. https://doi.org/10.17576/jsm-2020-4907-08

Riss, T. L., Moravec, R. A., & Niles, A. L. (2011). Cytotoxicity testing: Measuring viable cells, dead cells, and detecting mechanism of cell death. *Methods in Molecular Biology (Clifton, N.J.), 740*, 103–114. https://doi.org/10.1007/978-1-61779-108-6_12

Savic, S., Petrovic, S., & Knežević-Jugović, Z. (2026). Separation strategies for polyphenols from plant extracts: Advances, challenges, and applications. *Separations, 13*(2), 46. https://doi.org/10.3390/separations13020046

Sette, P., Mattson, M. G., Schebor, C., & Salvatori, D. (2025). Strategies for bioactive compound recovery from grape and apple wastes: Traditional and emerging technologies to reach zero waste discharge. *Biomass Conversion and Biorefinery, 15*, 28877–28894. https://doi.org/10.1007/s13399-024-05630-1

Shakoor, R., Hussain, N., Younas, S., & Bilal, M. (2023). Novel strategies for extraction, purification, processing, and stability improvement of bioactive molecules. *Journal of Basic Microbiology, 63*(3–4), 276–291. https://doi.org/10.1002/jobm.202200401

Shoji, T., Akazome, Y., Kanda, T., & Ikeda, M. (2004). The toxicology and safety of apple polyphenol extract. *Food and Chemical Toxicology, 42*(6), 959–967. https://doi.org/10.1016/j.fct.2004.02.008

Shu, P., Fan, S., Liu, S., Meng, Y., Wang, N., Guo, S., … Huang, J. (2025). Ultrasound-assisted deep eutectic solvent extraction of flavonoids from Cercis chinensis seeds : Optimization, Kinetics and Antioxidant Activity. *Separations, 12*(10), 269. https://doi.org/10.3390/separations12100269

Sugiyama, H., Akazome, Y., Shoji, T., Yamaguchi, A., Yasue, M., Kanda, T., & Ohtake, Y. (2007). Oligomeric procyanidins in apple polyphenol are main active components for inhibition of pancreatic lipase and triglyceride absorption. *Journal of Agricultural and Food Chemistry, 55*(11), 4604–4609. https://doi.org/10.1021/jf070569k

Tasaki-Handa, Y. (2021). Unusual ion-exchange selectivity in crystalline coordination polymers accompanied by structural change of the framework. *Bunseki Kagaku, 70* (10.11), 593–599. https://doi.org/10.2116/bunsekikagaku.70.593

Tedesco, I., Spagnuolo, C., Russo, G. L., Russo, M., Cervellera, C., & Moccia, S. (2021). The pro-oxidant activity of red wine polyphenols induces an adaptive antioxidant response in human erythrocytes. *Antioxidants, 10*(5), 800. https://doi.org/10.3390/antiox10050800

Tjandrawinata, R. R., Arnamalia, A., Warmiko, H. D., Permatasari, H. K., Taslim, N. A., Hardinsyah, H., & Nurkolis, F. (2026). Metabolomics, chemometrics, in silico and in vitro analyses reveal functional food phytochemicals of Indonesian spices for antioxidant, anticancer, anti-aging, and anti-obesity potential. *European Food Research and Technology, 252*. https://doi.org/10.1007/s00217-025-04928-2

Valentin-Severin, I., Le Hegarat, L., Lhuguenot, J. C., Le Bon, A. M., & Chagnon, M. C. (2003). Use of HepG2 cell line for direct or indirect mutagens screening: Comparative investigation between comet and micronucleus assays. *Mutation Research - Genetic Toxicology and Environmental Mutagenesis, 536*(1–2), 79–90. https://doi.org/10.1016/S1383-5718(03)00031-7

Villamil-Galindo, E., & Piagentini, A. (2024). Green solvents for the recovery of phenolic compounds from strawberry (Fragaria x ananassa Duch) and apple (Malus domestica) agro-industrial bio-wastes. *Revista de La Facultad de Ciencias Agrarias, 56* (1), 149–160. https://doi.org/10.48162/rev.39.131

Vinci, M., Gowan, S., Boxall, F., Patterson, L., Zimmermann, M., Court, W., … Eccles, S. A. (2012). Advances in establishment and analysis of three-dimensional tumor spheroid-based functional assays for target validation and drug evaluation. *BMC Biology, 10*, 29. https://doi.org/10.1186/1741-7007-10-29

Walkowiak-Tomczak, D., Idaszewska, N., Łysiak, G. P., & Bieńczak, K. (2021). The effect of mechanical vibration during transport under model conditions on the shelf-life, quality and physico-chemical parameters of four apple cultivars. *Agronomy, 11*(1), 81. https://doi.org/10.3390/agronomy11010081

Walzl, A., Unger, C., Kramer, N., Unterleuthner, D., Scherzer, M., Hengstschläger, M., … Dolznig, H. (2014). The resazurin reduction assay can distinguish cytotoxic from cytostatic compounds in spheroid screening assays. *SLAS Discovery, 19*(7), 1047–1059. https://doi.org/10.1177/1087057114532352

Wang, H., Wu, Z., & Cheng, J. (2019). Protective effect of apple phlorizin on hydrogen peroxide - induced cell damage in HepG2 cells. *Journal of Food Biochemistry, 43*, Article e13052. https://doi.org/10.1111/jfbc.13052

Wolfe, K., Wu, X., & Liu, R. H. (2003). Antioxidant activity of apple peels. *Journal of Agricultural and Food Chemistry, 51*(3), 609–614. https://doi.org/10.1021/jf020782a

World Health Organization. (2024). Obesity: Health consequences of being overweight. Available at: https://www.who.int/news-room/questions-and-answers/item/obesity-health-consequences-of-being-overweight. Accessed on 20 July 2026.

Xia, W., Song, B., Li, T., & Liu, R. H. (2024). Phytochemical profiles, antioxidant activities, and synergistic antiproliferative effects of blueberry and apple peel extracts. *Journal of the Science of Food and Agriculture, 104*(2), 737–745. https://doi.org/10.1002/jsfa.12964

Xiang, Y., Lai, F., He, G., Li, Y., Yang, L., Shen, W., … Zhang, Y. (2017). Alleviation of Rosup-induced oxidative stress in porcine granulosa cells by anthocyanins from red-fleshed apples. *PLoS ONE, 12*(8), Article e0184033. https://doi.org/10.1371/journal.pone.0184033

Zadeh, N. S., & Zeppa, G. (2022). Recovery and concentration of polyphenols from roasted hazelnut skin extract using macroporous resins. *Foods, 11*(13), Article 1969. https://doi.org/10.3390/foods11131969

Zanchi, D., Konarev, P. V., Tribet, C., Baron, A., Svergun, D. I., & Guyot, S. (2009). Rigidity, conformation, and solvation of native and oxidized tannin macromolecules in water-ethanol solution. *Journal of Chemical Physics, 130*(24). https://doi.org/10.1063/1.3156020